RSC Advances

PAPER

View Article Online
View Journal | View Issue



Cite this: *RSC Adv.*, 2016, **6**, 77717

# Dual inhibitors of epidermal growth factor receptor and topoisomerase IIα derived from a quinoline scaffold†

Monika Chauhan,[a] Gaurav Joshi,[a] Harveen Kler,[a] Archana Kashyap,[a] Suyog M. Amrutkar,[b] Praveen Sharma,[c] Kiran D. Bhilare,[b] Uttam Chand Banerjee,[b] Sandeep Singh[c] and Raj Kumar*[a]

Received 10th June 2016
Accepted 4th August 2016

DOI: 10.1039/c6ra15118c

www.rsc.org/advances

Based on the quinazoline bearing EGFR inhibitors, a series of thirty four compounds having a quinoline scaffold were synthesised and evaluated *in vitro* for EGFR kinase inhibitory activity. A structure–activity relationship study revealed that 2,4-bis(arylamino) substituted quinolines possessed better anti-EGFR kinase activity. Compounds **3f** and **3m** emerged as potent EGFR kinase inhibitors (200 and 210 nM, respectively) and showed excellent anticancer activity at the micromolar level against a panel of cancer cell lines comparable to erlotinib. Furthermore, representative compounds inhibited the human topoisomerase IIα selectively and catalytically, did not intercalate with DNA, increased intracellular ROS concentration (except **3m**) and altered the mitochondrial membrane potential of the cancer cells. Cell cycle analysis and annexin-V staining in a lung cancer cell line showed that the compounds delayed cell cycle progression by inducing cell cycle arrest and subsequent apoptosis at the G1 phase. The facts were further corroborated through molecular modeling studies.

## Introduction

The epidermal growth factor receptor (EGFR) belongs to a family of tyrosine kinases and is overexpressed and mediates growth of a variety of cancers, especially lung, breast, ovary, *etc.* through upregulated downstream cell signalling.[1,2] It is a clinically useful and druggable anticancer target and its inhibitors inhibit autophosphorylation either by binding to its extracellular growth factor binding domain (mabs) or intracellular ATP-binding site (nibs *i.e.* small molecules).[3,4] Several chemical scaffolds such as 4-aminoquinazolines,[5] pyridopyrimidines,[6] benzamides,[7] indolinones[8] and pyrrolotriazines[9] targeting its ATP-binding domain have been disclosed. Out of all the classes, 4-anilinoquinazoline is the most studied and explored and is present in FDA approved drugs such as gefitinib, erlotinib and lapatinib.[4,10] Human DNA topoisomerases comprised of Topoisomerase I (TopoI) and Topoisomerase II (TopoII) are validated targets in oncology,[11,12] highly expressed in many cancers and are involved in maintaining DNA topology, repair and religation of DNA. TopoI breaks the single strand of DNA whereas TopoII relaxes the super coiled DNA by breaking double strands of phosphate backbone of the DNA and needs ATP.[13] It has been revealed that both TopoI and TopoII interact with EGFR in a variety of cancer; brain, breast, ovarian, colorectal, gastric, *etc.* *via* different mechanisms leading to development of drug resistance.[10] Thus designing a dual inhibitor of EGFR and TopoI and or II might be an effective strategy to combat cancer.

Interaction model of gefitinib/erlotinib and EGFR ATP kinase domain yielded 3-cyanoquinoline derivatives (*e.g.* pelitinib).[14] Through our previous experiences in the field of anticancer drug discovery[15–24] and development[25] and earlier work on quinoline derivatives,[17,26] we herein propose the design of EGFR inhibitors (Fig. 1) having 4-amino-3-nitroquinoline scaffold (**1**) assuming that (a) replacement of C2–H (**1**) with an halogen atom (**2**) might reduce metabolism[27] and increase protein–ligand complex stability;[28] (b) an amino aryl/alkyl moiety (**3**; forming C2–N bond) might occupy extra space of ATP-binding pocket[29] and able to bind with mutant EGFR also and solve the issue of acquired resistance[30,31] and further the role of a bulkier group (**4**; forming C2-aryl bond) *via* Suzuki coupling and an amino at C-3 position on the EGFR inhibitory activity. With this background, we herein report the synthesis and detail biological evaluation of **1**, **2**, **3**, **4** and other compounds to generate structure–activity relationship, their mechanistic interventions derived through target based EGFR,

[a]*Laboratory for Drug Design and Synthesis, Centre for Pharmaceutical Sciences and Natural Products, Central University of Punjab, 151001, Bathinda, India. E-mail: raj.khunger@gmail.com; rajcps@cup.ac.in; Fax: +91-1636-236564; Tel: +91-0164-2864215*

[b]*Department of Pharmaceutical Technology (Biotechnology), National Institute of Pharmaceutical Education and Research (NIPER), S. A. S. Nagar, Sec 67, Mohali, 160062, Punjab, India*

[c]*Centre for Human Genetics and Molecular Medicine, Central University of Punjab, 151001, Bathinda, India*

† Electronic supplementary information (ESI) available: Spectral data of some representative compounds are given. See DOI: 10.1039/c6ra15118c

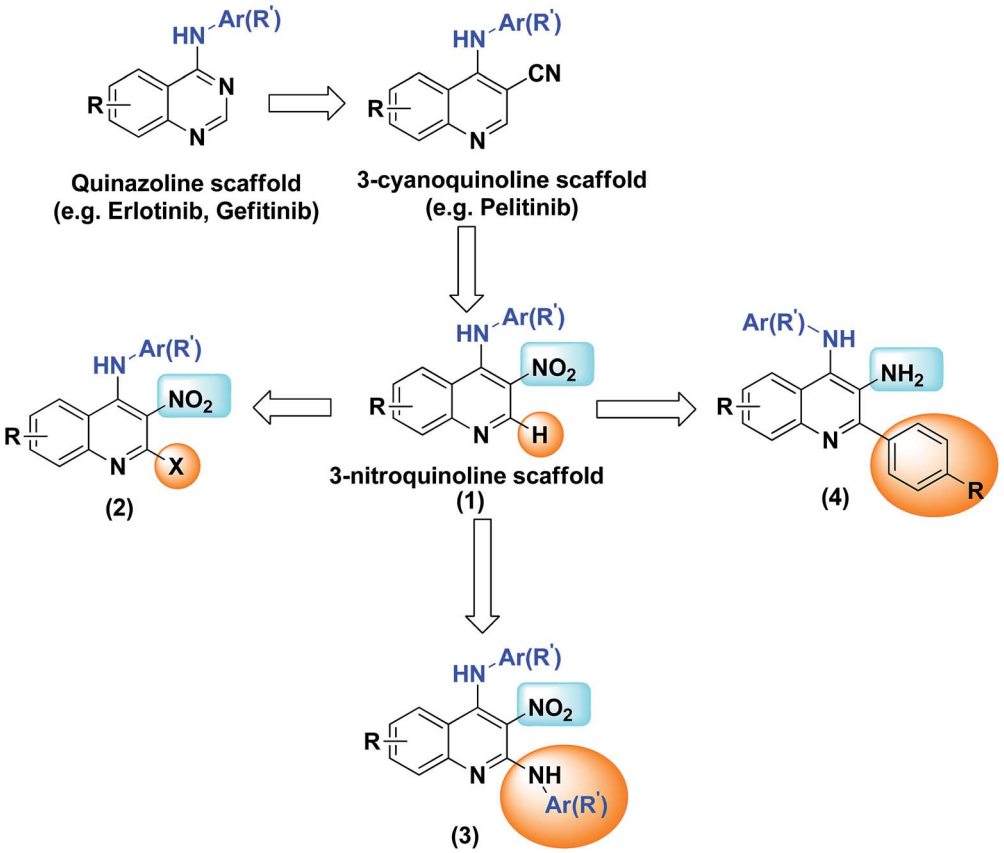


Fig. 1 Design of target compounds as new EGFR inhibitors (**1–4**).

TopoII and I inhibitory activities, intracellular reactive oxygen species (ROS) generation, mitochondrial destabilisation and apoptotic potentials and cell cycle analysis along with the reasons for the studies. Molecular docking methods further supported the results.

## Results and discussion

### Synthesis

Briefly, synthesis of representatives target compounds **1a–1c** and **1d** (Scheme 1) was accomplished from veratraldehyde (**5a**), and benzaldehyde (**5b**), respectively as a starting material. Compound **5** upon nitration yielded **6** which was oxidized to carboxylic acid (**7**). **7** underwent reduction (**8**), condensation with nitromethane under basic condition (**9**) followed by cyclisation to afford 3-nitroquinolin-4-ol (**10**).

**10** was converted into **11** which was further utilized to synthesize the final compounds by substituting with aromatic amines.[32] *N*-Oxide derivative (**1c**) of **1b** was synthesized *via* oxidation using hydrogen peroxide in the presence of acetic acid which was further brominated (**2a**) using NBS in THF (Scheme 1).

Preparation of target compounds **2b–2k** and **3a–3l** was achieved by the synthesis (previously reported)[17] of 3-nitroquinoline-2,4-diol (**13**) from quinoline-2,4-diol (**12**) which was further treated with $PhPOCl_2$ to obtain 2,4-dichloro-3-nitroquinoline (**14**).[17] **14** underwent $S_NAr$ with various aryl/aryl alkyl anilines to synthesize final compounds (Scheme 2).

Formation of **4a** and **4b** was routed *via* Scheme 3 which involves reduction of *N*-benzyl-2-chloro-3-nitroquinolin-4-amine (**2b**) to 2-chloro-3-nitroquinolin-4-amine (**15**) which was further treated with boronic acids to yield the final compounds. Surprisingly, reaction of 4-acetylphenyl boronic acid with **15** yielded debenzylated but a Suzuki coupled product **4a**. However, this was not the case when **15** was reacted with 3-chlorophenyl boronic acid.

In order to observe the effect of 4-amino aryl/arylalkyl substituent on EGFR inhibitory activity, **5a** and **5b** devoid of above said substituent(s) were synthesized by reacting **18** with 1-naphthalene boronic acid and 4-acetylphenyl boronic acid, respectively under Suzuki coupling conditions (Scheme 4).

All the unreported final compounds were fully characterized by melting point, IR, NMR and HRMS/CHNS analysis.

### Biological studies

**EGFR kinase inhibitory and antiproliferative activities.** To study the EGFR kinase inhibitory activity, the investigational compounds were screened for inhibition of ATP dependent phosphorylation of EGFR (Invitrogen catalogue no. PV3193). This assay is based on an enzymatic reaction in which auto-phosphorylation and signalling activity of the EGFR is measured. The inhibitory effect on kinase was measured

 

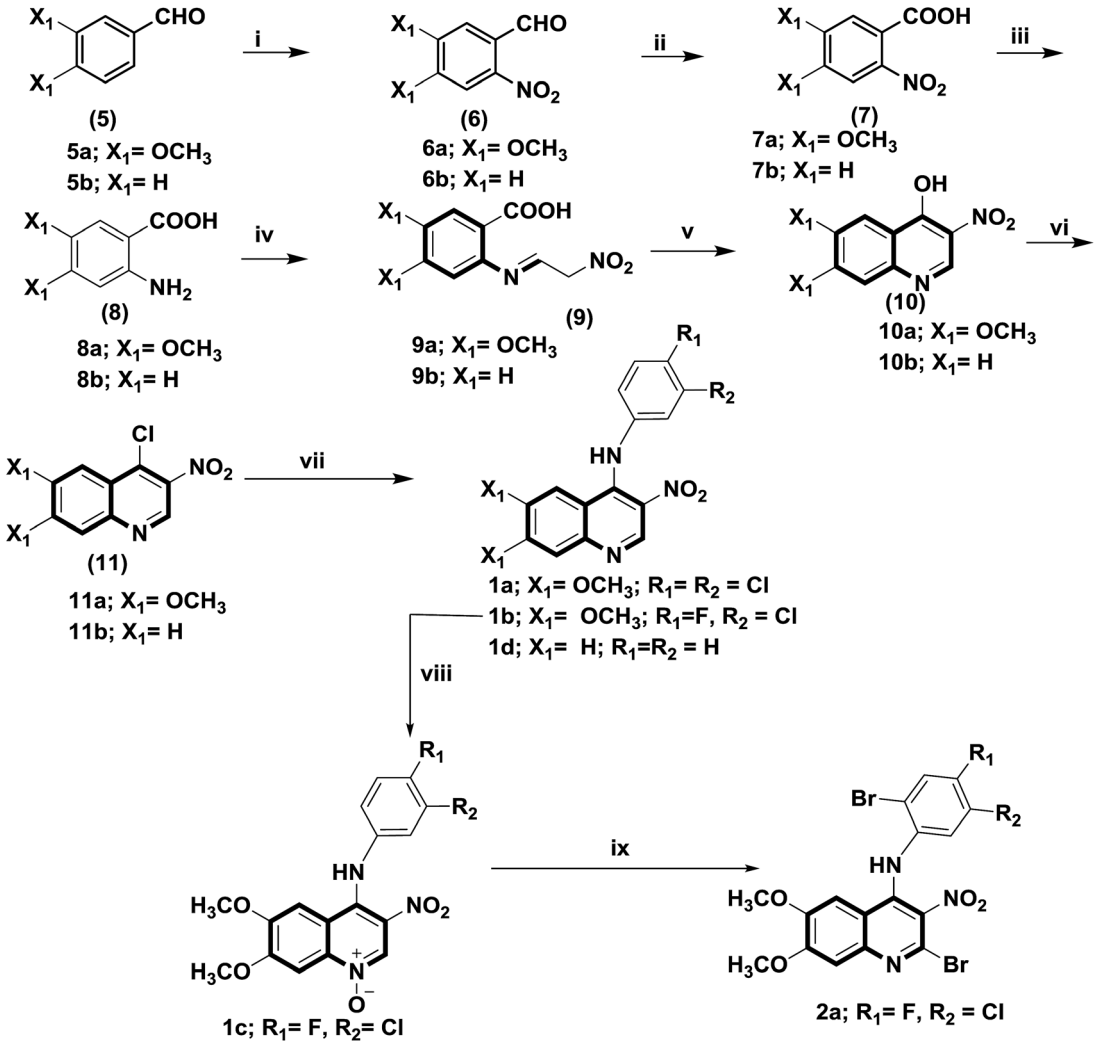


Scheme 1 Reagents and conditions: (i) fuming $HNO_3$/conc. $H_2SO_4$; (ii) 10% $KMnO_4$; (iii) Fe/$CH_3COOH$, reduction; (iv) $CH_3NO_2$/NaOH; (v) $(CH_3CO)_2O$/$CH_3COOK$; (vi) $POCl_3$, reflux; (vii) $PhNH_2$/MeOH, MW, 10 min, 80 °C; (viii) $H_2O_2$, $CH_3COOH$, 48 h; (ix) NBS/THF, reflux, 24 h.

spectrophotometrically at 400 nm, 445 nm and 520 nm respectively. Erlotinib was used as a positive control for the inhibition test. The results are collected in Table 1. Compounds **2a**, **2b**, **2f** and **2g** showed low micromolar EGFR inhibitory activity whereas compounds **3e–g**, **3i**, **3j** and **3m** exhibited activity in nanomolar range. Compounds **3m** and **3f** showed comparable EGFR inhibitory activity to erlotinib. Further, the most active EGFR inhibitors **3e–g**, **3i**, **3j** and **3m** were screened against a panel of cancer cell lines (Table 2); EGFR over-expressing human lung (A-549 and H-460), colon (HCT-116-wild type and HCT-116-p53 null) and prostate (PC-3). Compounds **3f**, **3g**, **3i** and **3j** inhibited the growth of lung cancer cell lines with $IC_{50}$ values (A-549) of 6.5 μM, 8.2 μM, 7.5 μM and 7.1 μM (H-460), respectively. Whereas **3e** and **3m** were active against colon cancer cell line (HCT-116-p53 null; $IC_{50}$ values of 5.1 μM and 4.8 μM, respectively). Practically all the above compounds were inactive prostate (PC-3) cancer cell line. Results of HCT-116 p53 null cell line indicated p53 independent mechanism of action.

No significant cytotoxicity towards normal cells (buccal cavity cells) with the above compounds at the highest concentration of 100 μM was observed (Fig. 2A). We further evaluated the synthetics **3m**, **3f**, **3g**, **3i**, **3j** and **3e** for their cytotoxic potential against Human Peripheral Blood Mononuclear Cells (hPBMCs) at 25 μM concentration. Erlotinib was used as positive control (Fig. 2B). To our interest, compound **3m** exhibited no significant cytotoxicity toward PBMCs even at the highest concentration of 25 μM. Erlotinib exhibited the acute cytotoxicity this concentration.

**Real time and RT-PCR assay.** As shown earlier, these compounds possess EGFR inhibitory potential *in vitro*, we selected few downstream targets of EGFR (twist and c-Fos) whose mRNA expression is dependent of EGFR activation. As per the available literature EGFR inhibition leads to up-regulation of twist (anti-apoptotic),[33] while c-Fos (apoptotic) is down regulated.[34] A549 cells were treated with 5 mM of compounds **3m**, **3f** and erlotinib followed by RT-PCR as well as real time PCR analysis. The RT-PCR results show that treatment

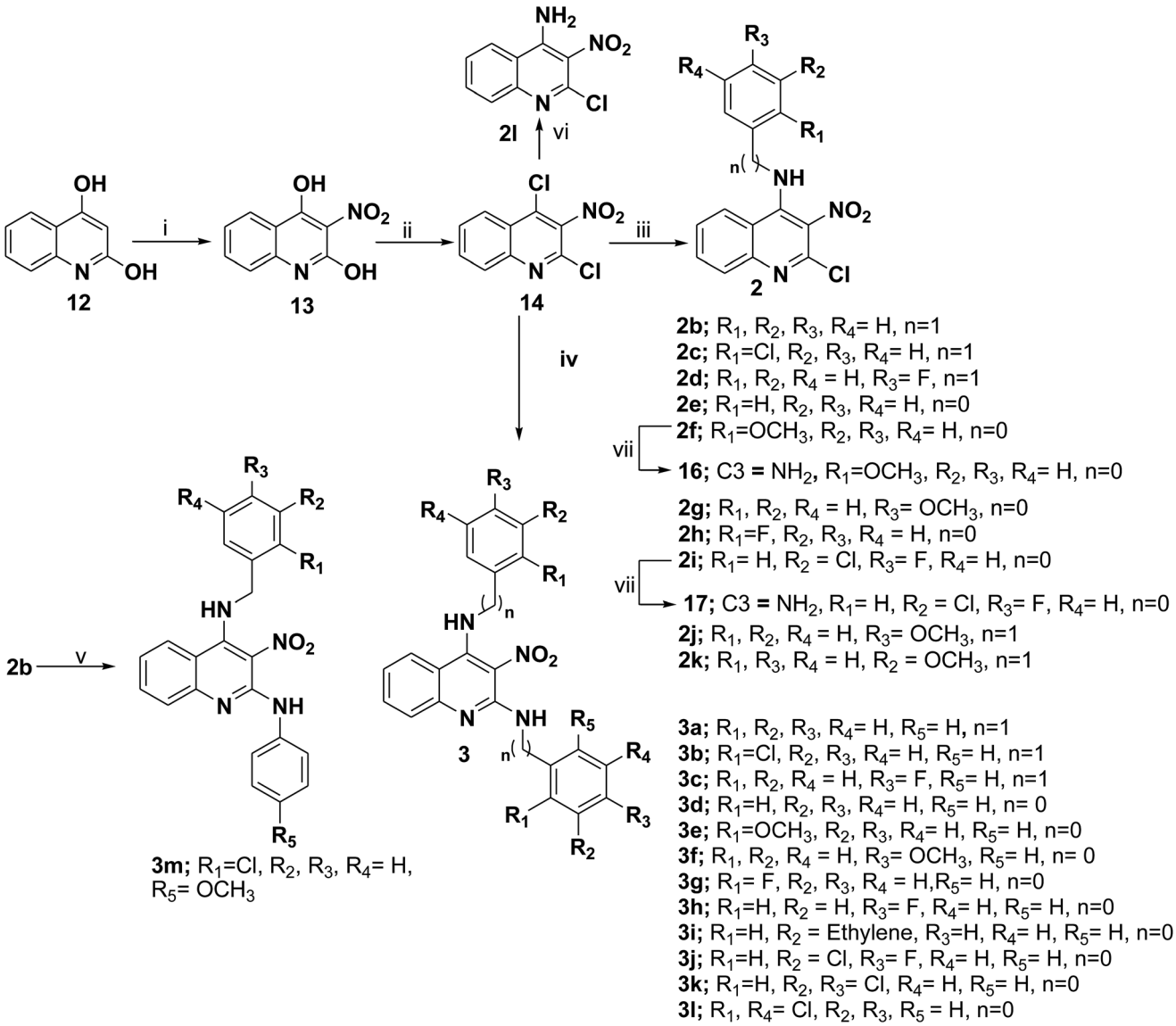


Scheme 2 Reactions conditions: (i) conc. $HNO_3$, $CH_3COOH$, reflux; (ii) $PhPOCl_2$, 140 °C, 4 h; (iii) aryl amine (1 equiv.), $Et_3N$, water, MW, 120 °C, 10–20 min; (iv) aryl amine (2 equiv.), $Et_3N$, water, MW, 120 °C, 10–20 min; (v) *p*-anisidine, MW, 25 min; (vi) $NH_3$ aq., 6 h, rt; (vii) Sn/HCl, MeOH, reflux, 6 h.

with both the compounds as well as erlotinib leads to down-regulation of c-Fos expression while twist expression is elevated (Fig. 3A) similar results were observed when samples were tested using real time PCR (Fig. 3B). These results show that expression of c-Fos and twist are modulated by treatment with these compounds *via* inhibition of EGFR activity.

**Structure–activity relationships (SAR).** Some general trends about structure–activity relationships noticed from these studies on the target compounds (Table 2) are as follows: (a) compounds having no aryl amine or arylalkyl amine substitution (**5a** and **5b**) or only $-NH_2$ substitution (**2l**, **4a** and **4b**) at C-4 position were inactive against EGFR kinase; (b) in general compounds having halogen substitution at C-2 position (**2a**, **2b**, **2f**, **2g** and **2h**) were found to be more active than with no substitution *i.e.* C-2–H (**1a–c**); (c) however, replacement of C2–halogen with arylalkyl amine (**3a–b**, **3h**) caused drop in activity whereas substitution with arylamino group enhanced the activity (**3e–g**, **3i**, **3j** and **3m**); (d) replacement of $NO_2$ at C-3 position with $NH_2$ group resulted in decrease of inhibitory activity (**4a–b**, **5a–b** and **15–17**) highlighting the role of nitro group in receptor binding; (e) in general compounds having C-2 and C-4 substitution with arylalkyl amines were less active than arylamine. The best activity was obtained when C-2 was bearing aryl amine and C-4 was having arylalkyl amine (**3m**).

## Topoisomerase assays

Recently it has been reported that quinazoline based EGFR inhibitors such as gefitinib and erlotinib also bind to topoisomerases.[35] We also reviewed the cross-talks of EGFR and topoisomerases which have been seen in various cancer including brain, breast, ovarian, colorectal, gastric, *etc.*[10]

 

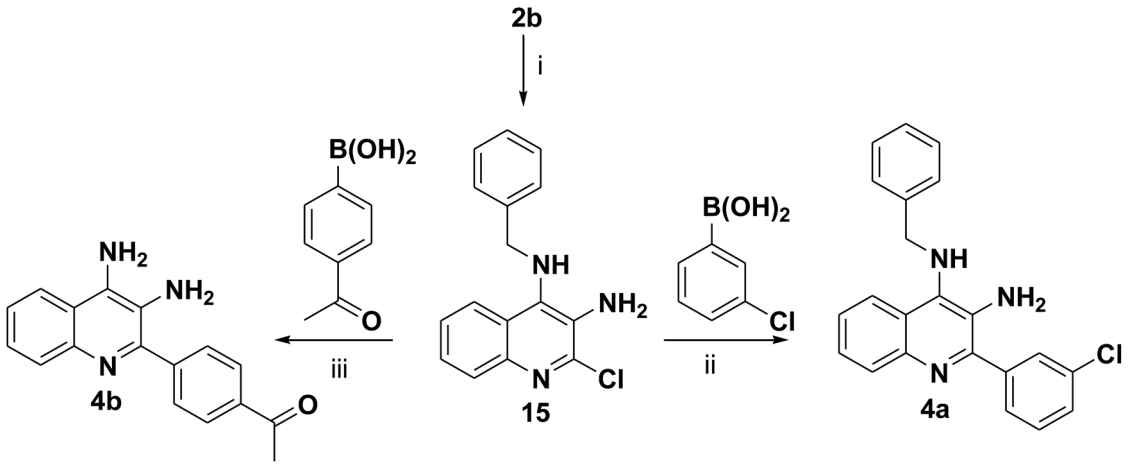


Scheme 3 Reactions conditions: (i) Sn/HCl, MeOH, reflux, 1 h; (ii) 3-chlorophenylboronic acid, $Pd(OAc)_2$, water, rt, stir, $N_2$; (iii) 4-acetylboronic acid, $Pd(OAc)_2$, water, rt, $N_2$.

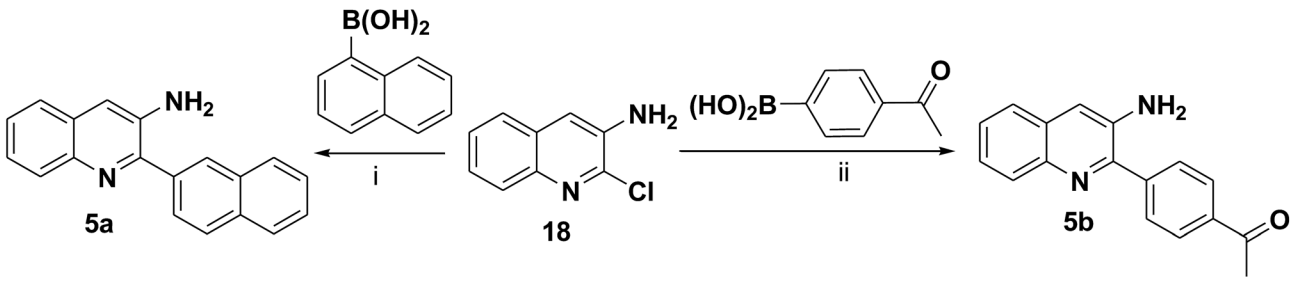


Scheme 4 Reactions conditions: (i) 1-naphthaleneboronic acid, $Pd(OAc)_2$, water, rt, $N_2$; (ii) 4-acetylboronic acid, $Pd(OAc)_2$, water, rt, $N_2$.

Therefore, to study the topoisomerase inhibitory potential of target compounds, the representative compounds **3a**, **3f** and **3m** (bis-aminated) and **2g** (mono-aminated) were chosen and screened for the following assays.

**Inhibition of hTopoIIα mediated kDNA decatenation assay.** Compounds **2g**, **3a**, **3f** and **3m** were evaluated for inhibition of hTopoIIα mediated kDNA decatenation. In this assay, kinetoplast DNA (kDNA) and etoposide (known TopoII inhibitor) acted as a substrate and standard inhibitor, respectively. Incubation of kDNA with human topoisomerase IIα forms decatenated products, these products can be discerned by agarose gel electrophoresis.[36] Compound **2g** demonstrated relatively more inhibition of decatenation than etoposide (**E**) (Fig. 4A and B).

**Inhibition of hTopoI mediated kDNA relaxation assay.** Compounds **2g**, **3a**, **3f** and **3m** were tested for inhibition of hTopoI mediated relaxation. Herein, camptothecin was taken as a standard (known TopoI inhibitor) while negatively supercoiled DNA (SC DNA) was used as a substrate. Incubation of SC DNA with human topoisomerase-I leads to the formation of Nck (nicked), Rel (relaxed), and SC (supercoiled) DNA isoforms. As compared to camptothecin, relatively insignificant inhibition of hTopo-I mediated relaxation was observed with compound **2g**, **3a**, **3f** and **3m** (Fig. 4C).

Further, to investigate the ability of compounds **2g**, **3a**, **3f** and **3m** to intercalation into DNA was studied by DNA intercalation assay.

**DNA intercalation assay.** In the gel electrophoresis, ethidium bromide (DNA intercalators) retards the movement of SC DNA. The compounds **2g**, **3a**, **3f** and **3m** exhibited no such retardation of DNA movement confirming the DNA non-intercalating nature of the investigated compounds (Fig. 5).

## Molecular docking

***In silico* studies on ATPase binding site of EGFR.** As compounds **3m** and **3f** emerged to be the top EGFR inhibitors *in vitro*, and to theoretically investigate the binding pattern of the compounds with EGFR, these were docked into the ATPase binding site of EGFR (PDB entry: 1M17).[29] The significant interactions between the ligands and the target protein were scored using GLIDE 6.1 module of Schrödinger Suite. The validation of the docking protocol was accomplished by removing co-crystal ligand (erlotinib) and docking back into the active site of EGFR kinase domain. The observed X-ray crystallographic conformation and the docked conformation of erlotinib displayed a good agreement between their positioning and showed a similar binding pose. The root mean square deviation (RMSD) was computed to be 0.014 Å indicating that the parameters for docking protocol are acceptable. The binding model of erlotinib presented that it gets placed into the cavity formed by Leu 694, Leu 764, Phe 699, Pro 770, Val 702, Leu 753, Ala 719 and exhibited hydrogen bond interaction with Met 769. The interaction of Met 769 with erlotinib has also been reported in literature.[37]

Table 1 EGFR inhibitory activity of the target compounds

| Cd | EGFR inhibitory activity; $IC_{50}$[a] (μM) |
|---|---|
| **1a** | 28.1 ± 0.2 |
| **1b** | 30.5 ± 0.4 |
| **1c** | 32 ± 0.3 |
| **2a** | 18 ± 0.1 |
| **2b** | 17 ± 0.6 |
| **2c** | 20 ± 0.2 |
| **2d** | 22 ± 0.7 |
| **2e** | 24 ± 0.2 |
| **2f** | 9 ± 0.4 |
| **2g** | 12 ± 0.3 |
| **2h** | 19 ± 0.8 |
| **2i** | 25 ± 0.2 |
| **2j** | 28 ± 0.1 |
| **2k** | 29 ± 0.5 |
| **2l** | >100 |
| **3a** | 49.12 ± 0.2 |
| **3b** | 42.08 ± 0.3 |
| **3c** | 38.10 ± 0.1 |
| **3d** | 39.21 ± 0.3 |
| **3e** | 280 ± 0.2 nM |
| **3f** | 220 ± 0.4 nM |
| **3g** | 450 ± 0.2 nM |
| **3h** | >100 |
| **3i** | 480 ± 0.6 nM |
| **3j** | 250 ± 0.5 nM |
| **3k** | >100 |
| **3l** | >100 |
| **3m** | 200 ± 0.1 nM |
| **4a** | 40.3 ± 0.3 |
| **4b** | 42.1 ± 0.1 |
| **5a** | 56.2 ± 0.6 |
| **5b** | 58.3 ± 0.2 |
| **15** | >100 |
| **16** | 59.2 ± 0.1 |
| **17** | 54.8 ± 0.7 |
| Erlotinib | 240 ± 0.1 nM |

[a] Values are derived from averaging three independent experiments and each experiment was done in triplicate.

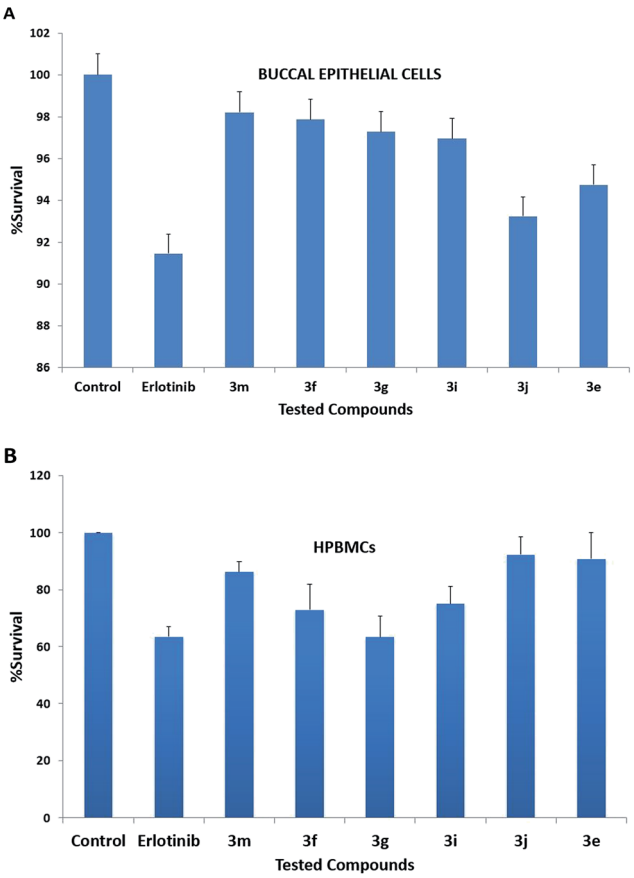


Fig. 2 (A) Percent survival of buccal cavity cells at 100 μM in response to treatment with **3m**, **3f**, **3g**, **3i**, **3j** and **3e** and erlotinib (positive control) for time duration of 48 h. (B) Percent survival of human peripheral blood mononuclear cells in response to treatment with **3m**, **3f**, **3g**, **3i**, **3j** and **3e** and erlotinib (positive control) at concentrations of 25 μM for time duration of 48 h. Data is expressed as mean values ± S.D. of three independent experiments.

The superimposition of the co-crystallized ligand with **3m** and **3f** displayed that the two compounds occupy the binding domain in a manner similar to erlotinib (Fig. 6A).

Compounds **3m** and **3f** presented a *G* score of −5.519 and −4.760, respectively (Table 3). The interaction figure of compound **3m** revealed that the two amino acids; Met 769 and Lys 721 stabilized the compound by hydrogen bond and π–cation interactions, respectively. A hydrogen bond at a distance of 2.1 Å was formed between the backbone amine

Table 2 Antiproliferative activity of most potent EGFR inhibitors (**3e–g**, **3i**, **3j** and **3m**)

| Cd | A549 | H460 | HCT-116 p53 (null) | HCT-116 p53 (wild type) | PC-3 |
|---|---|---|---|---|---|
| $IC_{50}$[a] (μM) | | | | | |
| **3e** | 18.2 ± 0.1 | 13.2 ± 0.3 | 5.1 ± 0.2 | >25 | 13.0 ± 0.2 |
| **3f** | 6.5 ± 0.2 | >25 | 23.2 ± 0.5 | >25 | >25 |
| **3g** | 8.2 ± 0.5 | 21.2 ± 0.3 | >25 | >25 | 22.3 ± 0.3 |
| **3i** | 7.5 ± 0.3 | 17.8 ± 0.2 | 12.6 ± 0.4 | 12.4 ± 0.2 | >25 |
| **3j** | >25 | 7.1 ± 0.5 | >25 | 17.3 ± 0.3 | >25 |
| **3m** | 10.5 ± 0.1 | 23.6 ± 0.1 | 13.6 ± 0.5 | 14.6 ± 0.2 | 15.5 ± 0.5 |
| Erl[b] | 12 ± 0.2 | 8.3 ± 0.5 | 7.0 ± 0.2 | —[c] | —[c] |

[a] Values are derived from averaging three independent experiments and each experiment was done in triplicate. [b] Erlotinib (positive control). [c] Not tested.

 

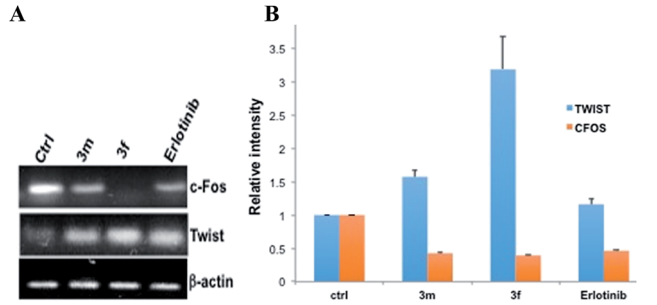


Fig. 3 (A) Reverse Transcriptase-PCR (RT-PCR) for c-Fos and twist mRNA after treatment with compounds **3m** and **3f** while erlotinib is used as positive control. β-Actin in the figure is the loading control. (B) Real time PCR analysis of c-Fos and twist upon treatment with compounds **3m** and **3f** while erlotinib is used as positive control.

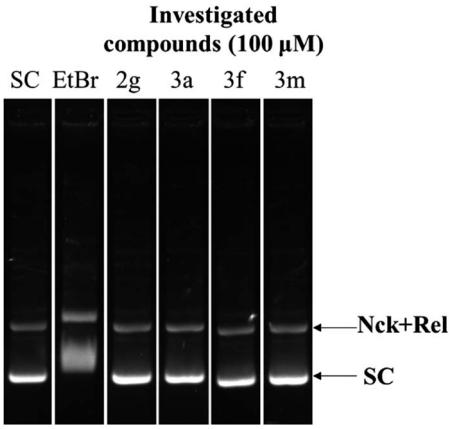


Fig. 5 DNA intercalation assay: SC DNA (pUC19) was incubated with 1 μg $mL^{-1}$ of ethidium bromide, 100 μM of investigated compounds (**2g**, **3a**, **3f** and **3m**).

group of Met 769 and oxygen of the nitro group. In addition, the amine group of the methoxyaniline ring was involved in hydrogen bonding with the backbone carbonyl group of Met 769 ($d = 2.0$ Å). The π–cation interaction was observed between the chlorobenzene ring and ammonium group in Lys 721 ($d = 5.0$ Å). A hydrogen bond interaction was seen between HOH 10 and amine group of chlorobenzyl amine ring ($d = 3.6$ Å). The

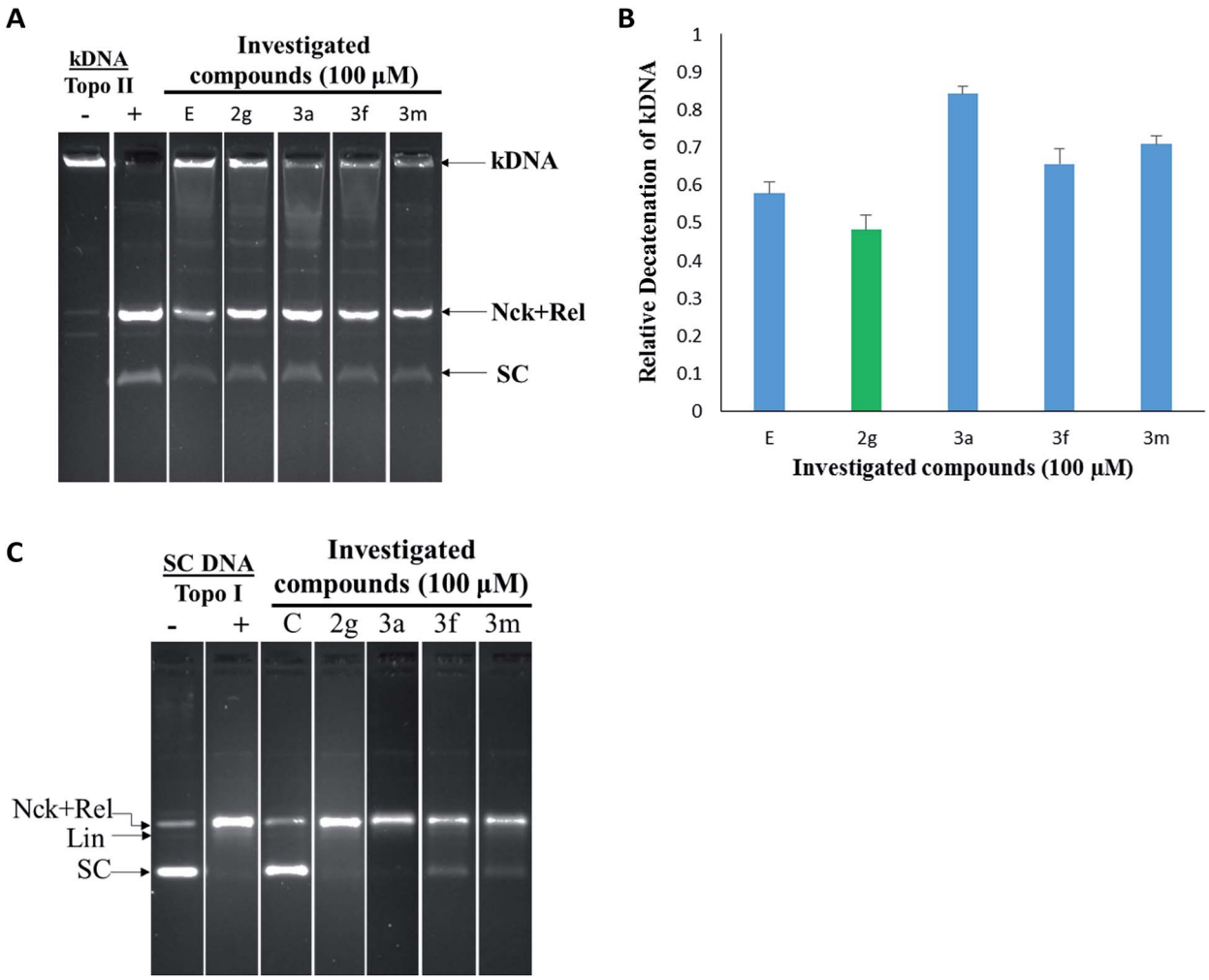


Fig. 4 (A) Decatenation assay: kDNA was treated with hTopoIIα in presence of either 100 μM etoposide (**E**) or investigated compounds **2g**, **3a**, **3f** and **3m**. (B) Quantification of product formed in kDNA decatenation assay. (C) Topoisomerase-I relaxation assay: hTopo-I act on negatively supercoiled DNA in the presence of either 100 μM camptothecin (C) or compounds **2g**, **3a**, **3f** and **3m**.

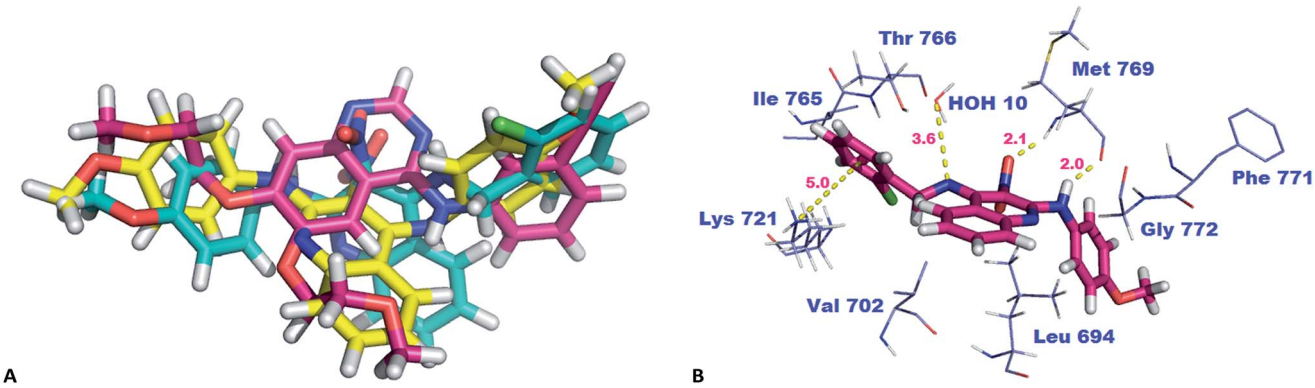


Fig. 6 (A) Superimposed binding orientation of compounds **3m** (blue), **3f** (yellow) and erlotinib (pink) within the ATP binding site of 1M17. (B) Active 3-D binding model of **3m** as revealed from Glide docking in the ATP binding site of EGFR (PDB 1M17).

compound could also show hydrophobic interactions with Leu 820, Cys 773, Leu 764, Leu 694, Ala 719, Met 742 (Fig. 6B).

***In silico* studies on ATPase domain of hTopoII.** The biological studies showed that the representative compounds **3a** (bis-aminated) and **2g** (mono-aminated) exhibited TopoII inhibitory activity. These compounds were then docked into the ATPase domain of hTopoII (PDB entry: 1ZXM)[38] to identify the key interactions. The docking procedure was carried out for the target compounds into hTopoII using GLIDE 6.1. The validation process was executed by re-docking the phosphoaminophosphonic acid–adenylate ester (ANP) into the of ATPase domain of hTopoII. The predicted conformation of ANP was observed to be similar to that of the co-crystal ligand with a RMSD of 0.024 Å. The interaction model of ANP with ATPase domain displayed that the carbonyl group of Asn 120 showed hydrogen bonding with the amino group of adenine moiety. Additionally, the nitrogens showed hydrogen bonding with the water molecules present in the side chain; HOH 931, HOH 933 and HOH 924. The side chain residue Ser 149, exhibited hydrogen bond interaction with the hydroxyl group of ribose unit. Further, the oxygen atoms in the three phosphate groups showed hydrogen bond interactions with the backbone residues; Gly 166, Ala 167, Asn 163, Tyr 165, and with the side chains residues; Ser 148, Lys 168, Glu 87, Asn 91, and Gln 376. These also formed coordinate bonds with Mg 904. The Mg cation shows an octahedral geometry by forming three point contacts with the phosphate groups of ANP, HOH 927, HOH 928 and the carbonyl oxygen of Asn 91.[16] The Walker A motif comprising of residues; Arg 162, Asn 163, Gly 164, Tyr 165, Gly 166 and Ala 167 remains conserved and is vital for binding of the catalytic inhibitors to ATPase domain.[21] Compound **2g** exhibited the highest docking score of −5.383. Furthermore, the superimposition of ANP with **2g** and **3a** indicated that the three occupy the ATPase binding site in an identical fashion (Fig. 7A). The binding model of the top scoring compound, **2g** revealed that the oxygen of the nitro group showed hydrogen bond interaction with the backbone amino group of Ser 149 ($d = 2.5$ Å) and the side chain hydroxyl group of Ser 148 ($d = 2.7$ Å). The other oxygen formed a salt bridge with ammonium ion of Lys 168 ($d = 3.5$ Å). The methoxy benzene ring showed π–cation interactions with Mg 903 ($d = 2.2$ Å). Also, the oxygen of the methoxy group formed a hydrogen bond with the backbone amine group of Arg 162 ($d = 2.2$ Å). The compound, however, could show hydrophobic interactions with Tyr 34, Phe 142, Tyr 165, Ile 141, Ile 217, and Ile 125 and polar interactions with Thr 147, Asn 163, Gln 376, Asn 150, Thr 215 and Asn 91 (Table 3 and Fig. 7B).

Table 3 Docking parameters and some important key interactions observed with amino acid residues of EGFR and Topo II active site and inhibitors

| EGFR active site | | | |
|---|---|---|---|
| Cd | Glide score | Binding energy | Important interaction |
| **3m** | −5.519 | −71.8889 | Met 769, Lys 721, HOH 10 |
| **3f** | −4.760 | −65.8714 | Met 769 |

| Topo II active site | | | |
|---|---|---|---|
| Cd | Glide score | Interaction with Mg ion | Important interaction |
| **2g** | −5.383 | π–Cation | Arg 162, Lys 168, Ser 148, Ser 149 |
| **3a** | −3.843 | π–Cation | Phe 142 |

## DHE based reactive oxygen species (ROS) assay

**Dose-dependent increase in reactive oxygen species (ROS) generation in cancer cells.** Majority of anticancer agents induce significant changes in the ROS level of cells.[15,16,39] In order to assess the effects of the synthetics on ROS level and to conclude whether the anticancer effect of compounds is mediated by free radicals,[40] ROS assay was performed.

Some representative compounds **2g**, **2e**, **3a**, **3m** and **3f** were assessed for the ROS study in A-549 lung cancer cell line using DHE based fluorescent detection system (Fig. 8). The results showed that there is concentration dependent increase in ROS levels in the treated cells while compound **3m** showed no significant change in ROS levels.

 

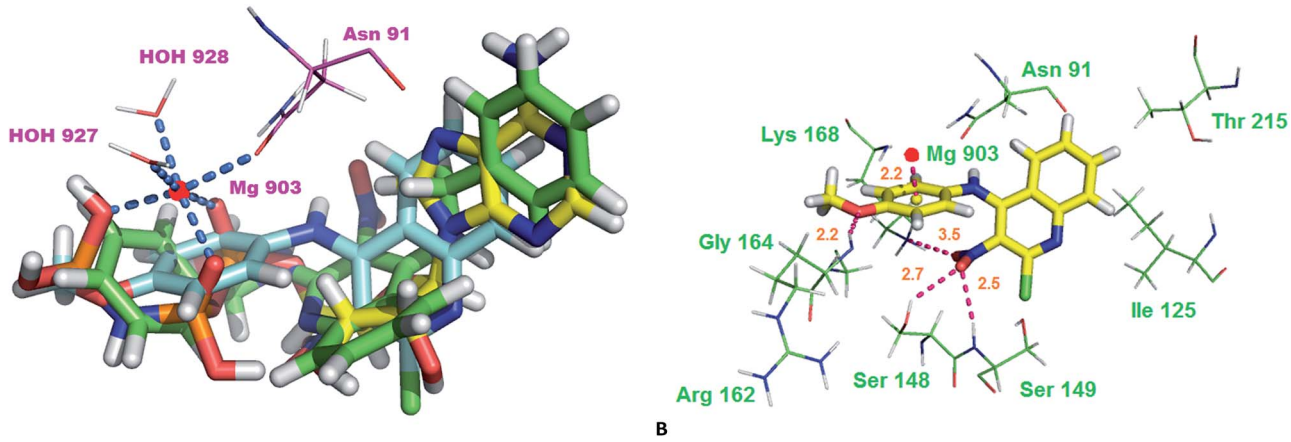


Fig. 7 (A) Superimposed binding orientation of compounds **3a** (green), **2g** (blue) and ANP (yellow) within the ATPase binding domain of hTopoII (PDB 1ZXM). (B) Active binding model of **2g** as revealed from Glide docking in the ATPase binding domain of hTopoII (PDB 1ZXM).

### Mitochondrial membrane integrity (JC-1) assay

**Increased depolarization in mitochondrial membrane of cancer cells.** Deviations in mitochondrial membrane potential are largely associated with the increase in ROS levels that triggers membrane depolarization and lead to release of cytochrome-c into cytoplasm, thus induce intrinsic pathway of apoptosis.[15,41] The compounds **2g**, **2e**, **3a**, **3m** and **3f** were assayed for their effect on mitochondrial membrane potential of A-549 lung cancer cells. JC-1 dye was used to measure membrane potential of the mitochondria;[15,21,42] the results showed that there is steady decrease in OD590/OD527 ratio signifying increased mitochondrial membrane depolarization at 1 and 5 μM (Fig. 9). Most of the compounds showed higher relative ratio at 25 μM which may be attributed to the fact that higher concentrations are very toxic to the cells and perhaps that's the reason behind skewed relative ratios.

**Apoptosis and cell cycle analysis.** In order to further explore the mechanism underlying the antiproliferative effects of compounds, we measured the effect of representative compound **3m** and erlotinib (a positive control) on A549 cell proliferation by examining the expression of annexin V using Muse™ Annexin V and Dead Cell kit to detect phosphatidyl serine membrane translocation which is considered as major hallmark of late stages apoptosis. As shown in Fig. 10, treatment with **3m** at concentration of 1 and 5 μM resulted in increase in early (26.03% and 36.73%, respectively) and late apoptosis (4.29% and 17.37%, respectively) of cells as

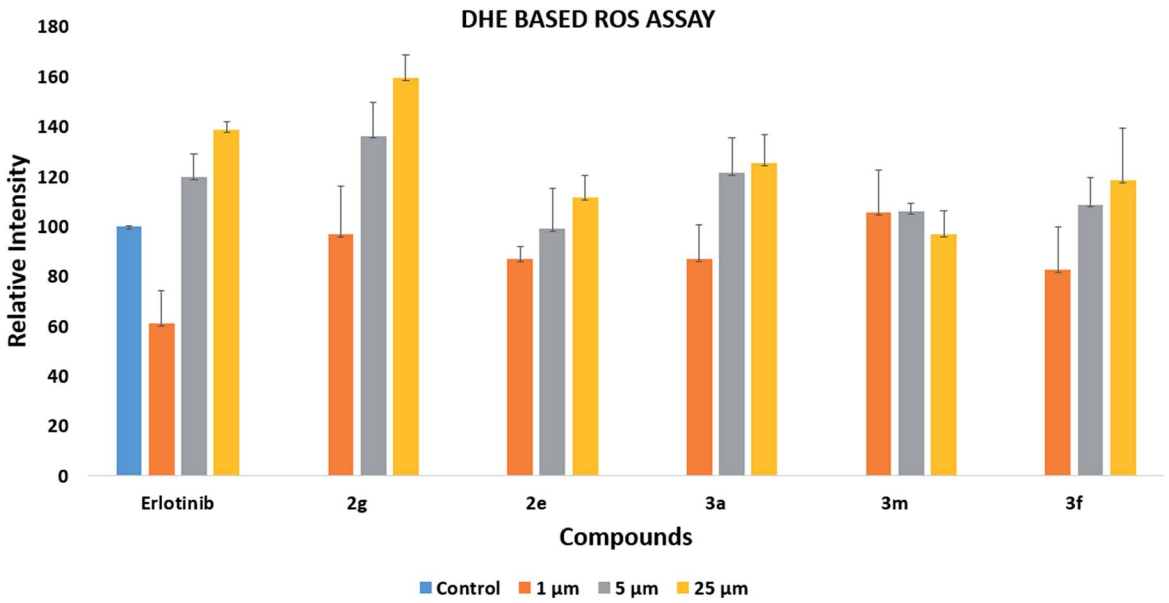


Fig. 8 DHE based assay to measure intracellular reactive oxygen species (ROS) induced in A-549 cell line by **2g**, **2e**, **3a**, **3m**, **3f** and erlotinib.

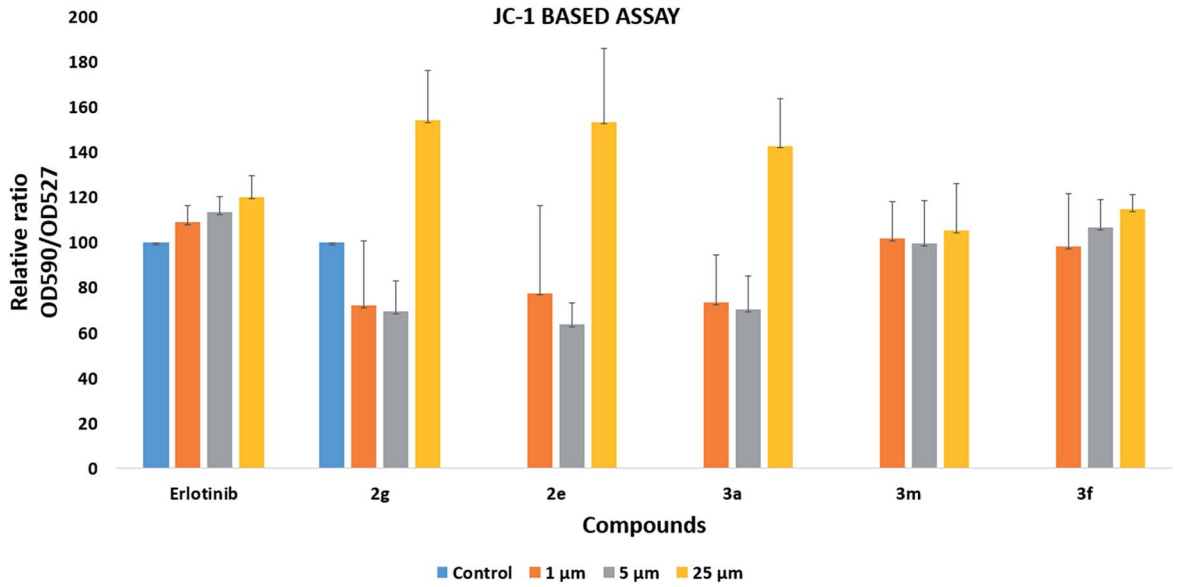


Fig. 9 JC-1 dye based assay to measure the mitochondrial membrane potential altered in A-549 cell line by **2g**, **2e**, **3a**, **3m**, **3f** and erlotinib.

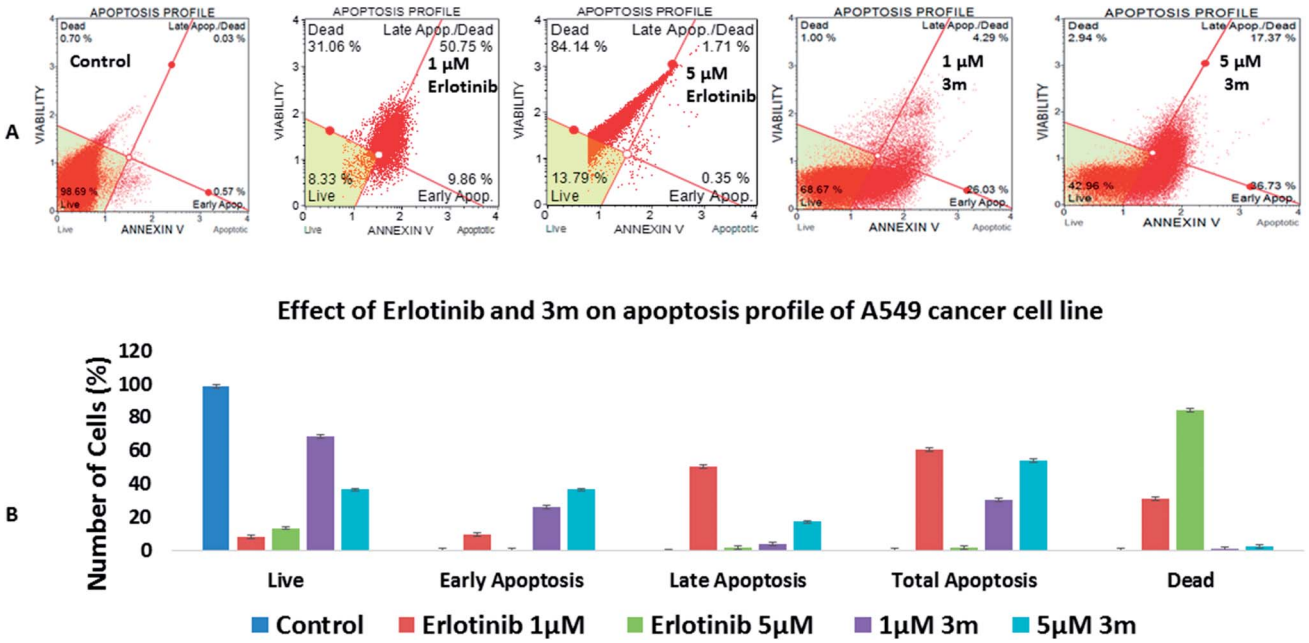


Fig. 10 Effect of compound **3m** and erlotinib on A549 cancer cell line apoptosis. (A) Apoptosis was measured using annexin V stain utilising MUSE™ flow cytometer. (B) The bar graph represents the quantitative analysis of percentage of total apoptotic cells.

compared to control used during the experimental conditions.

Further, cell cycle analysis was performed on BD C6 accuri flow cytometer using propidium iodide. A549 cell line was treated with **3m** and erlotinib (a positive control) at 1, 5 and 25 μM concentrations for 24 h. Treatment with **3m** at 25 μM resulted in increase in fraction of cells (49.61%) arrested in G1 phase from control (33.59%) (Fig. 11B). We next treated **3m** with A549 cell line at 1, 5 and 25 μM concentrations for 48 h and found out DNA content index (Fig. 12) using MUSE™ cell analyser. The DNA contents of the live population were 62.2%, 24.7%, and 10.8% for untreated cells, and 99.4%, 0.6%, and 0% for **3m**-treated cells at 25 μM, respectively for G0/G1, S and G2/M phase. Taken together, the results of apoptosis and DNA content analysis suggest that these compounds delay the cell cycle progression by arresting cell cycle at G1 phase. However, erlotinib (Fig. 11A) did not exhibit the similar pattern.[43]

 

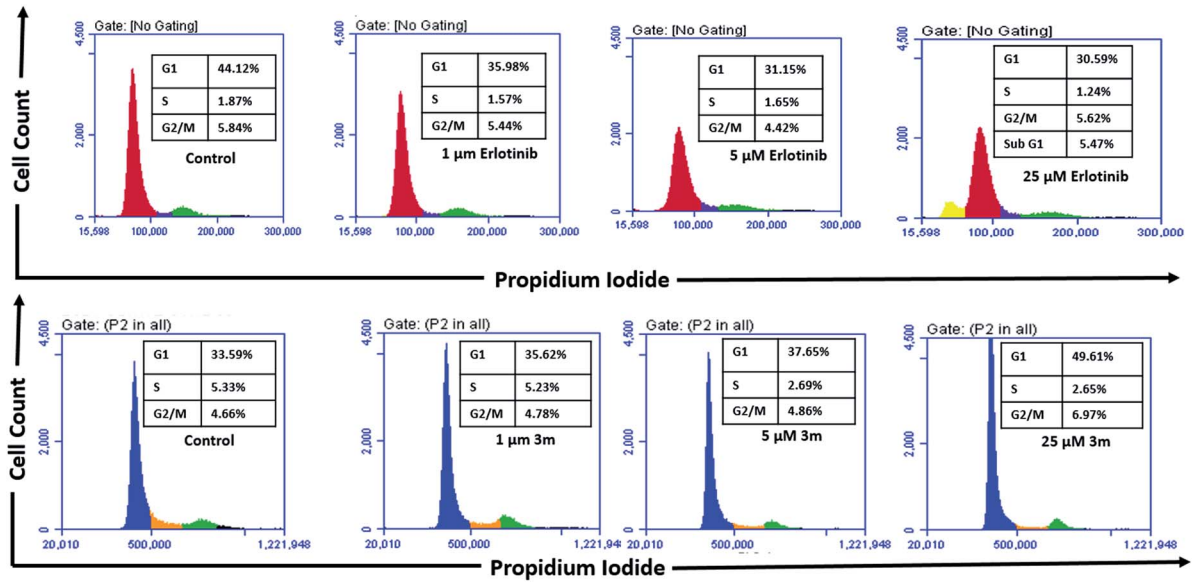


Fig. 11 Cell cycle analysis using BD C6 flow cytometry. The study was conducted for compound **3m** and erlotinib (a positive control) using EGFR positive A549 cancer cell line that showed profound apoptosis causing G1 phase arrest.

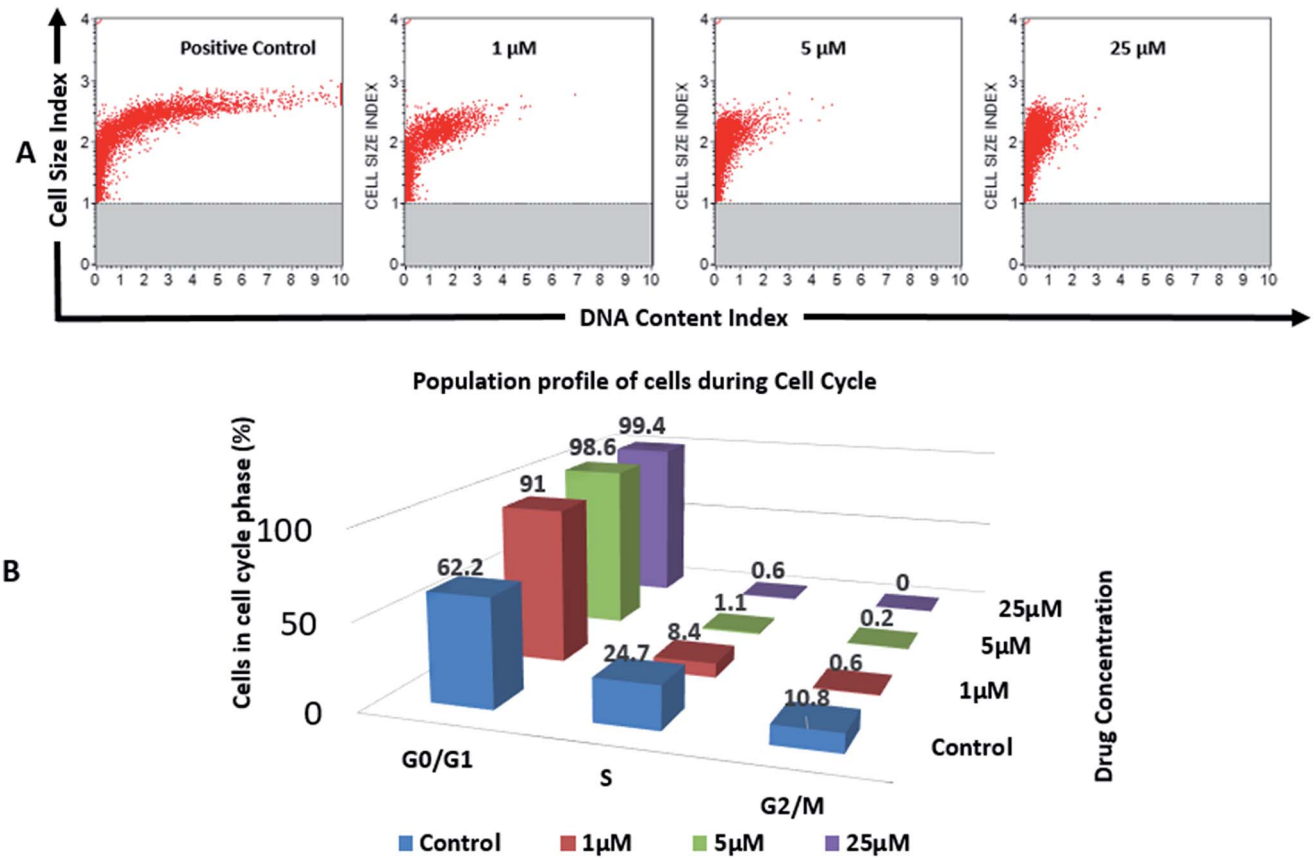


Fig. 12 (A) DNA content index analysis using MUSE™ cell analyser. The study was conducted for compound **3m** using A549 cancer cell line that induced profound G1 phase arrest. (B) The bar graph represents the percent DNA content at various cell cycle stages of A549 cancer cells-untreated and treated with **3m**.

## Conclusions

In summary, quinoline based compounds were designed, synthesised and assessed for their potential EGFR kinase inhibitory and antiproliferative activities in cancer cell lines. The compounds exhibited anti-EGFR activity at nanomolar and antiproliferative activity at low micromolar range. As previously reported in case of quinazoline based EGFR inhibitors, the present compounds were also able to inhibit the TopoIIα selectively and catalytically. The above observations were further supported by molecular docking studies. The compounds were not found to be DNA intercalators. Further investigations on molecular mechanisms revealed that title compounds were able to induce intracellular ROS generation and alter the mitochondrial membrane potential of cancer cells. Apoptosis analysis in A549 cell lines suggested that these compounds were able to disrupt the cell cycle progression and induce cell cycle arrest at G1 phase. Real time and RT-PCR data suggest that EGFR downstream targets are affected upon treatment with the compounds indicating their EGFR inhibitory potential. These observations over all suggest that anticancer activity of the compounds is a result of involvement of multiple pathways comprised of free radical generation, EGFR and TopoIIα inhibition leading to cancer cell death. We will publish further lead optimisation of potent compounds and their detailed antitumor potential in due course.

## Experimental

### Synthesis

The reagents for the synthesis of compounds were purchased from Sigma-Aldrich, Loba and CDH, India and used without further purification. All yields refer to isolated products after purification. Products were characterized by spectroscopic data (IR, NMR, MS spectra and CHNS analysis). NMR experiments were measured in $CDCl_3$/$d_6$-DMSO relative to TMS (0.00 ppm). IR (KBr pellets) spectra were recorded on a Fourier transform infrared (FT-IR) thermo spectrophotometer. Melting points were determined in open capillaries and were uncorrected. All the target compounds were characterised by IR, NMR, mass and or elemental analyses.

### Synthesis of 4,5-dimethoxy-2-nitrobenzaldehyde (6a)

Veratraldehyde (500 mg) was reacted with conc. nitric acid (8 mL) at 0 °C. The mixture was stirred for 2 h at rt. The progression of reaction was monitored *via* TLC. Reaction mixture was poured on cold ice water and filtered. Product was used for next step without further purification.[32]

Yield: 89%; yellow colour compound; mp: 132–145 °C; $^1$H NMR (400 MHz, $CDCl_3$): $\delta$ 10.36 (1H, s), 8.15 (1H, s), 8.03 (1H, s), 3.4 (6H, s, $OCH_3$).

### Synthesis of 2-nitrobenzaldehyde (6b)

Concentrated $HNO_3$ (5 mL) was cautiously added to the benzaldehyde at 0 °C. Then the mixture was stirred for 40 min at 15 °C. On pouring the reaction mixture into ice water, insoluble material precipitated. The precipitate was filtered out to afford the crude product.[32]

Yield: 90%; yellow colour compound; mp: 42 °C; IR (KBr, $cm^{-1}$): CHO (1685), C–N (1227), C–H aromatic (3122), C=C aromatic (1574), $NO_2$ (1337 symmetric), $NO_2$ (1500 asymmetric).

### Synthesis of 4,5-dimethoxy-2-nitrobenzoic acid (7a)

2.1 g of 4,5-dimethoxy-2-nitrobenzaldehyde (**6a**) was added to 6 mL of acetone in hot water and stirred for 1 h. 5 mL of $KMnO_4$ was added to the reaction mixture. Resulting mixture was filtered. Filtrate was concentrated to remove the acetone and was cooled off. Dil. HCl was added in the concentrated mixture slowly with the cooling until the pH of solution becomes acidic. White precipitates of the compound were filtered and washed with water.

Yield: 79%; white solid; $^1$H NMR (400 MHz, $d_6$-DMSO, TMS = 0) $\delta$: 11.00 (1H, s), 8.48 (1H, s), 8.35 (1H, s), 3.73, (6H).

### Synthesis of 2-nitrobenzoic acid (7b)

2-Nitrobenzaldehyde (1 g; **6a**) was dissolved in acetone (12 mL) and hot water (10 mL). To this reaction mixture, 10% $KMnO_4$ was added and the mixture was stirred for 1 h. Then the reaction mixture was filtered and the filtrate was concentrated to remove the acetone. HCl was added slowly with cooling until the insoluble white solid material precipitated (90% yield) and was used for next step.[32]

Yield: 90%; white flakes; mp: 145 °C; IR ($cm^{-1}$): 1681 (C=O), 1292 (C–N), 3089 (C–H aromatic), 1606 (C=C aromatic), 1575 ($NO_2$).

### Synthesis of 2-amino-4,5-dimethoxybenzoic acid (8a)

500 mg of **7a** was added to acetic acid (6 mL). The reaction mixture was heated at 90 °C and iron powder (5 equiv., 150 mg) was added partially to reaction mixture in 20 min. Resulting mixture was stirred for 45 minutes and reaction mixture was filtered. The solid compound was filtered and dried.[32]

Yield: 80%; brown solid; IR (KBr, $cm^{-1}$): 3322 & 3432 ($NH_2$ stretch), 1468 (C=C aromatic), 1683 (COOH), 2825 ($OCH_3$ stretch).

### Synthesis of 2-aminobenzoic acid (8b)

2-Nitrobenzoic acid (1 g; **7b**) was dissolved in an appropriate amount of acetic acid (20 mL) and the mixture was stirred for about 30 min at 90 °C. To this reaction mixture, iron powder was added with stirring. After 2 h, the reaction mixture was filtered and the filtrate was poured into 10% aqueous hydrochloric acid solution and the insoluble material predicated. The residue was dissolved in hot water and 15% sodium hydroxide solution was added until the pH was 12. After cooling to room temperature, the insoluble material precipitated and was used for next step without further purification.[32]

Yield: 72%; brown solid; mp: 146–148 °C; $^1$H NMR (400 MHz, $d_6$-DMSO): $\delta$ 11.00 (1H, s), $\delta$ 7.85 (1H, s), 7.02 (1H, s), 7.19 (1H, s), 6.84 (1H, s), 6.27 (2H, s).

 

### Synthesis of (*E*)-4,5-dimethoxy-2-((2-nitrovinyl)amino)benzoic acid (9a)

300 mg of dimethoxy benzoic acid was added in 8 mL of water with 0.3 mL of conc. HCl. 200 mg of NaOH was dissolved in 2 mL of water, and nitromethane was added (0.4 g) to the solution of sodium hydroxide and mixture was stirred for 1 h at 40 °C. Again nitromethane was added and mixture was stirred at 50 °C for 15–30 min. Reaction mixture was poured in ice water and conc. HCl was added until the pH of the mixture was 2, then this reaction mixture was added to the solution of benzoic acid. Reaction mixture was stirred at room temperature for 24 h. The organic layer was concentrated and dried.[32]

$^1$H NMR (400 MHz, $CDCl_3$, TMS = 0), $\delta$ = 13.19 (1H, d, $J$ = 16 Hz), 7.79–7.86 (1H, m), 7.49 (1H, d, $J$ = 16 Hz), 7.08 (1H, s), 6.64 (1H, d, $J$ = 8 Hz), 3.98 (3H, s), 3.87 (3H, s). $^{13}$C NMR (100 MHz, $d_6$-DMSO) $\delta$: 168.17, 153.67, 144.51, 136.81, 136.15, 112.95, 108.37, 112.95, 108.37, 98.04.

### Synthesis of (*E*)-2-((2-nitrovinyl)amino)benzoic acid (9b)

2.75 g of anthranilic acid in 25 mL of water was dissolved and 0.5 mL of conc. HCl was added. In another beaker, 1.3 g of NaOH in water at 0 °C was mixed. Nitromethane (0.7 g) was added to the solution of NaOH and stirred at 40 °C. After stirring the mixture for 15–20 min, again nitromethane (0.7 g) was added to this mixture. The reaction mixture was poured in ice water. Then this reaction mixture was added to the solution of anthranilic acid and water and was stirred for 24 h. The insoluble yellow material precipitated, product was filtered (90% yield) and dried and was used for next step without further purification.[32]

Light green solid; yield 82%; mp: 152 °C; IR (KBr, cm$^{-1}$): 1365 ($NO_2$), 1616 (C=N), 3122 (C–H aromatic), 1468 (C=C aromatic), 1683 (C=O); $^1$H NMR (400 MHz, $CDCl_3$, TMS = 0) $\delta$ = 13.08 (1H, d, $J$ = 12 Hz), 8.07–7.99 (1H, m), 7.90 (1H, dd, $J_{12}$ = 4 Hz, $J_{13}$ = 8 Hz), 7.65–7.53 (2H, m), 7.19–7.15 (1H, m), 6.68 (1H, d, $J$ = 4). $^{13}$C NMR (100 MHz, $d_6$-DMSO): 168.43, 140.68, 136.79, 134.11, 131.72, 123.04, 116.57, 114.72, 113.48.

### Synthesis of 6,7-dimethoxy-3-nitroquinolin-4-ol (10a)

**9a** acid was dissolved in minimum amount of acetic anhydride (approx. 5–7 mL) in 50 mL RBF and heated at 100–105 °C until a clear solution is obtained. Heating was then discontinued and potassium acetate (500 mg) was added. The reaction mixture was again refluxed for about 30 minutes, until solid started to precipitate. The reaction mixture was then cooled to room temperature and the residue was filtered. It was then washed with glacial acetic acid until the washing became colourless, and finally with cold water. The product was finally dried to get the crude product.[32]

$^1$H NMR (400 MHz, $CDCl_3$, TMS = 0) = 9.12 (1H, s), 7.56 (1H, s), 7.53 (1H, s).

### Synthesis of 3-nitroquinolin-4-ol (10b)

**9b** was dissolved in minimum amount of acetic anhydride (approx. 5–7 mL) in 50 mL RBF and heated at 100–105 °C until a clear solution is obtained. Heating was then discontinued and potassium acetate (500 mg) was added. The reaction mixture was again refluxed for about 30 minutes, until solid started to precipitate. The reaction mixture was then cooled to room temperature and the residue was filtered. It was then washed with glacial acetic acid until the washing became colorless, and finally with cold water. The product was finally dried to get the crude product and was used for next step without further purification.[32]

Light green solid; yield 80%; mp: 235–238 °C; IR (KBr, cm$^{-1}$): 1058 (C–N), 1632 (C=N), 3122 (C–H aromatic), 1599 (C=C aromatic), 1493 ($NO_2$ asymmetric), 1337 ($NO_2$ symmetric), 2825 ($OCH_3$ stretch). $^1$H NMR (400 MHz, $d_6$-DMSO, TMS = 0) $\delta$ = 9.10 (1H, s), 8.32 (1H, d, $J$ = 8 Hz), 7.69 (1H, d, $J$ = 8 Hz), 7.59–7.55 (1H, m), 7.32 (1H, t, $J_{12}$ = 4 Hz, $J_{23}$ = 8). $^{13}$C NMR (100 MHz, $d_6$-DMSO): 173.29, 168.89, 148.19, 147.04, 130.82, 129.32, 125.95, 125.38, 123.81.

### Synthesis of 4-chloro-6,7-dimethoxy-3-nitroquinoline (11a)

Phosphorous oxychloride (1 mL) was added to 3-nitroquinolin-4-ol (500 mg) with stirring. The reaction mixture was refluxed at 100 °C. After that the solvent was removed under the vacuum and the residue was poured over the crushed ice with stirring. The mixture was filtered, collected and dried to obtain the crude product and was used for next step after purification using flash chromatography.[32]

IR (KBr, cm$^{-1}$): 1218 (C–N), 1632 (C=N), 1492 ($NO_2$ asymmetric), 772 (C–Cl); $^1$H NMR (400 MHz, $CDCl_3$, TMS = 0) $\delta$ = 11.36 (1H, s), 8.38 (1H, d, $J$ = 4 Hz), 7.47 (1H, d, $J$ = 4 Hz), 3.89 (6H, s). $^{13}$C NMR (100 MHz, $d_6$-DMSO): 169.75, 168.33, 153.29, 143.32, 137.50, 112.89, 107.11, 102.95, 55.82, 55.69.

### Synthesis of 4-chloro-3-nitroquinoline (11b)

3-Nitroquinolin-4-ol (500 mg) was added to phosphorous oxychloride (1 mL) with stirring. The reaction mixture was refluxed at 100 °C. After that the solvent was removed under the vacuum and the residue was poured over the crushed ice with stirring. The mixture was filtered, collected and dried to obtain the crude product (80% yield) and was used for next step.[32]

Green solid; yield 80%; mp: >300 °C; $^1$H NMR (400 MHz, $d_6$-DMSO, TMS = 0) $\delta$ = 9.17 (1H, s), 8.48 (1H, q), 7.89–7.80 (2H, m), 7.56–7.50 (1H, m).

### General procedure for the synthesis of *N*-substituted-6,7-dimethoxy-3-nitro-*N*-quinolin-4-amine

To a reaction vial, a suspension of 4-dichloro-3-nitroquinoline (100 mg, 1 mmol) in methanol (1 mL) was added substituted aniline (1 equiv.) and the mixture was heated under microwave irradiation using Biotage initiator for 10 min at 80 °C. After the completion of the reaction (TLC), methanol was evaporated from mixture, extracted with ethylacetate, dried and purified *via* flash chromatography.

Physical data of unknown compounds of series 1 is given below.

**Synthesis of *N*-(3,4-dichlorophenyl)-6,7-dimethoxy-3-nitro-*N*-quinolin-4-amine (1a).** Dark yellowish colour; yield 76%; mp:

240 °C; IR (KBr, $cm^{-1}$): 2954 (C–H stretch), 1610 (C=N stretch), 1529 (C=C aromatic), 1218 (C–O stretch), 1259 (C–N stretch), 772 (C–Cl stretch). $^1$H NMR (400 MHz, $CDCl_3$, TMS = 0), 10.18 (1H, s), 9.36 (1H, s), 7.37 (1H, s), 7.22 (1H, dd, $J_{12}$ = 4 Hz), 7.16 (1H, t, $J_{12}$ = 8 Hz, $J_{23}$ = 8 Hz), 6.99–7.03 (1H, m), 6.82 (1H, s), 4.12 (3H, s), 3.49 (3H, s). HRMS (TOF-ESI) calcd for $C_{17}H_{13}Cl_2N_3O_4$, 393.03 $(M)^+$; observed: 394.058 $(M + 1)^+$.

**Synthesis of *N*-(4-flouro-3-chlorophenyl)-6,7-dimethoxy-3,4-diamine (1b).** Light brown solid; yield 80%; mp: 127 °C; IR (KBr, $cm^{-1}$): 2850 (C–H stretch), 1580 (C=N stretch), 1496 (C=C aromatic), 1260 (C–O stretch), 1219 (C–N stretch); $^1$H NMR (400 MHz, $CDCl_3$, TMS = 0), 10.11 (1H, s), 9.27 (1H, s), 7.16–7.14 (1H, m), 7.08 (1H, s), 6.92–6.96 (1H, m), 6.74 (1H, s), 3.41 (3H, s), 3.96 (3H, s); $^{13}$C NMR (100 MHz, $d_6$-DMSO): 56.41, 55.54, 105.50. 109.37, 112.77, 117.20, 117.42, 122.99, 123.05, 125.42, 137.96, 144.12, 145.04, 148.24, 148.69, 154.45, 154.53; HRMS (TOF-ESI) calcd for $C_{17}H_{13}ClFN_3O_4$, 377.06 $(M)^+$; observed: 378.0435 $(M + H)^+$.

**Synthesis of 4-((3-chloro-4-fluorophenyl)amino)-6,7-dimethoxy-3-nitroquinoline 1-oxide (1c).** 100 mg of *N*-(4-flouro-3-chlorophenyl)-6,7-dimethoxy-3,4-diamine (**1b**) was dissolved in acetic acid followed by addition of hydrogen peroxide (2 mmol). The reaction mixture was stirred for 48 h. The completion of reaction was monitored *via* TLC. The product was extracted with ethylacetate, dried and further purified *via* flash chromatography (4%).

Orange solid; yield 92%; mp: 130 °C; IR (KBr $cm^{-1}$): 2924 (C–H stretch), 1617 (C=N stretch), 1538 (C=C aromatic), 1216 (C–O stretch), 1461 (C–N stretch); $^1$H NMR (400 MHz, $CDCl_3$, TMS = 0), 10.10 ($D_2O$ exchangeable NH, s), 9.37 (1H, s), 7.43 (1H, s), 7.41 (1H, d, $J$ = 4 Hz), 7.26 (1H, m), 6.95 (1H, m), 6.94 (1H, s), 4.04 (3H, s), 3.50 (3H, s); Mass (EI): 393 $(M)^+$. Anal. found: C, 51.77; H, 3.43; N, 10.82. Calcd for $C_{17}H_{13}ClFN_3O_5$: C, 51.86; H, 3.33; N, 10.67.

**Synthesis of 3-nitro-*N*-phenylquinolin-4-amine (1d).** A mixture of 4-chloro-3-nitroquinoline (100 mg), aniline (500 μL) and methanol was heated under microwave for 10 min at 80 °C. The solvent was removed under vacuum and the mixture obtained was extracted with ethyl acetate. The organic layer was concentrated by rotary evaporator to obtain the crude product which was purified through column chromatography.

Light green solid; yield 89%; mp: 222 °C; $^1$H NMR (400 MHz, $d_6$-DMSO, TMS = 0), $\delta$ = 10.62 (1H, s), 9.47 (1H, s), 8.00 (1H, d, 8 Hz), 7.71–7.65 (2H, m), 7.44–7.36 (2H, m), 7.29–7.26 (1H, m), 7.21–7.15 (3H, m). $^{13}$C NMR (100 MHz, $d_6$-DMSO): 150.42, 146.95, 146.71, 140.95, 132.64, 130.34, 129.86, 128.51, 127.52, 126.47, 125.59, 123.50, 118.88. HRMS (TOF-ESI) calcd for $C_{17}H_{13}ClFN_3O_5$, 265.270 $(M)^+$; observed: 266.1729 $(M + H)^+$.

Physical data of unknown compound of series 2 is given below.

**Synthesis of 2-bromo-*N*-(2-bromo-3-chloro-4-fluorophenyl)-6,7-dimethoxy-3-nitroquinolin-4-amine (2a).** 100 mg of **1c** was dissolved in 1 mL of THF. Then NBS (1 equiv.) was added to the solution and refluxed for 24 h. Reaction was monitored *via* TLC. The precipitates were washed with isopropyl alcohol followed by ether. The product was purified *via* flash chromatography.

Brown solid; yield 70%; mp: 257 °C; IR (KBr $cm^{-1}$): 2921 (C–H stretch), 1495 (C=N stretch), 1580 (C=C aromatic), 1219 (C–O stretch). $^1$H NMR (400 MHz, $CDCl_3$, TMS = 0), 10.89 ($D_2O$ exchangeable NH, s), 8.40 (1H, s), 7.42 (1H, s), 7.19 (2H, s), 3.96 (3H, s), 3.90 (3H, s). Anal. found: C, 38.21; H, 2.41; N, 7.83. Calcd for $C_{17}H_{11}Br_2ClFN_3O_4$: C, 38.13; H, 2.07; N, 7.85;

**Synthesis of 3-nitroquinoline-2,4-diol (13).** **13** was synthesized using protocol reported in the literature.[17] Mp: 210–212 °C; IR (KBr, $cm^{-1}$): 3313 (OH stretch), 2850 (C–C stretch), 2350 (C=N stretch), 1522 ($NO_2$ stretch); $^1$H NMR ($CDCl_3$, 400 MHz, $\delta$ with TMS = 0): 12.00 (1H, s), 8.05–8.03 (1H, dd, $J_{12}$ = 1.2 Hz; $J_{13}$ = 8.4 Hz), 7.62–7.58 (1H, m), 7.35–7.33 (1H, d, $J$ = 8 Hz), 7.26–7.22 (1H, m); $^{13}$C NMR ($CDCl_3$, 100 MHz, $\delta$ with TMS = 0) $\delta$: 157.11, 155.78, 138.21, 132.98, 126.41, 124.41, 122.06, 115.76, 113.77; MS (ESI): $m/z$ = 207.1 $[M + 1]^+$.

**Synthesis of 2,4-dichloro-3-nitroquinoline (14).** **14** was synthesized using protocol reported in the literature.[17] Mp: 94–96 °C; IR (KBr, $cm^{-1}$): 1614 (C=N), 1490 (C=C), 1215 (C–N), 748 (C–Cl); $^1$H NMR ($CDCl_3$, 400 MHz, $\delta$ with TMS = 0): 8.28–8.26 (1H, dd, $J_{12}$ = 1.2 Hz; $J_{13}$ = 8.8 Hz), 8.13–8.10 (1H, d, $J$ = 8.4 Hz), 7.97–7.92 (1H, m), 7.83–7.79 (1H, m). $^{13}$C NMR ($CDCl_3$, 100 MHz, $\delta$ with TMS = 0) $\delta$: 147.3, 144.78, 141.3, 132.19, 129.6, 128.6, 125.5, 124.4.

**Synthesis of 2-chloro-3-nitroquinolin-4-amine (2l).** To a reaction vial, a suspension of **14** (240 mg, 1 mmol) in methanol (1 mL) was added aq. ammonia (2 equiv.) and the mixture was stirred for 6 h. After the completion of the reaction the product was extracted with ethyl acetate, evaporated and dried. The product was purified *via* flash chromatography.

Yield: 90%; brown solid; mp: 132–134 °C; $^1$H NMR ($CDCl_3$, 400 MHz, $\delta$ with TMS = 0): 7.94 (1H, dd, $J_{12}$ = 4 Hz; $J_{13}$ = 8 Hz), 7.70 (1H, dd, $J_{12}$ = 4 Hz; $J_{13}$ = 8 Hz), 7.49 (1H, d, $J$ = 8 Hz), 7.20 (1H, d, $J$ = 12 Hz). Anal. found: C, 48.38; H, 2.75; N, 18.83. Calcd for $C_{17}H_{13}ClFN_3O_5$: C, 48.34; H, 2.70; N, 18.79.

Physical data of unknown compound of series 3 is given below.

**Synthesis of $N^2$,$N^4$-bis(2,5-dichlorophenyl)-3-nitroquinoline-2,4-diamine (3l).** To a solution of 2,4-dichloro-3-nitroquinoline (100 mg, 0.41 mmol, 1 equiv.) in water (2 mL) were added triethylamine (0.6 mL, 0.49 mmol, 1.2 equiv.) and 2,4-dichlorobenzylamine (0.7 mL, 0.82 mmol, 2 equiv.). The reaction mixture was stirred for 20 min in biotage microwave synthesizer. After the completion of the reaction (TLC), solid product was extracted with ethyl acetate (10 mL × 3). Organics were washed with brine (10 mL × 3), dried over anhydrous $Na_2SO_4$ and evaporated under reduced pressure using rotary evaporator to obtain the product. The product was finally dried to get the pure product.

Yield: 90%; red solid; IR (KBr, $cm^{-1}$): 3196 (NH stretch), 1539 ($NO_2$ stretch), 857 (C–Cl stretch); $^1$H NMR ($CDCl_3$, 400 MHz) $\delta$: 10.28 ($D_2O$ exchangeable NH, s), 10.12 ($D_2O$ exchangeable NH, s), 7.71 (1H, d, $J$ = 8 Hz), 7.60–7.69 (1H, m), 7.52 (1H, d, $J$ = 4 Hz), 7.47 (1H, d, $J$ = 4 Hz), 7.29–7.32 (1H, dd, $J_{12}$ = 2.4, $J_{13}$ = 8 Hz), 7.25 (3H, m), 7.08–7.12 (2H, m), 7.01–7.08 (1H, m), 6.68 (1H, d, $J$ = 8 Hz). Anal. found: C, 51.09; H, 2.50; N, 11.39. Calcd for $C_{21}H_{12}Cl_4N_4O_2$: C, 51.04; H, 2.45; N, 11.34.

 

**Synthesis of $N^4$-benzyl-2-(3-chlorophenyl)quinoline-3,4-diamine (15).** To a suspension of *N*-benzyl-2-chloro-3-nitroquinolin-4-amine (**2b**) (250 mg, 1 mmol) in methanol (1 mL) was added Sn/HCl (2 equiv.) and the mixture was refluxed for 1 h. After the completion of the reaction (TLC), methanol was evaporated, compound was dried and purified through triturating with EtOAc and hexane mixture.

Yield: 30%; brown solid; mp: 172–174 °C; $^1$H NMR ($CDCl_3$, 400 MHz, $\delta$ with TMS = 0): 7.81 (1H, d, $J$ = 8 Hz), 7.56 (1H, d, $J$ = 8 Hz),7.46–7.48 (1H, m), 7.37–7.39 (5H, m), 6.94–6.91 (1H, m), 5.02 (1H, $D_2O$ exchangeable NH, s), 4.60 (2H, $D_2O$ exchangeable NH, s), 3.42 (2H, s). Anal. found: C, 67.79; H, 4.94; N, 14.88. Calcd for $C_{16}H_{14}ClN_3$: C, 67.72; H, 4.97; N, 14.81.

## General procedure for the synthesis of C-2 substituted quinolines

2-Chloro-3-aminoquinoline (100 mg, 1 mmol), substituted-arylboronic acid (1.2 mmol), and palladium acetate (0.02 mmol) were taken in water and stirred at room temperature under inert conditions (TLC). The reaction mixture was extracted with ethyl acetate (10 × 3 mL). Product was purified by column chromatography.

Physical data of unknown compounds of series 4 is given below.

**Synthesis of $N^4$-benzyl-2-(3-chlorophenyl)quinoline-3,4-diamine (4a).** Light yellow semi-solid; yield 47%; IR (KBr, $cm^{-1}$): 3200 (N–H stretch), 1639 (C=N stretch), 1544 (C=C aromatic), 550 (C–Cl stretch). $^1$H NMR ($CDCl_3$, 400 MHz) $\delta$: 8.12–8.09 (3H, m), 7.63–7.61 (2H, m), 7.50–7.48 (4H, m), 7.08 (1H, t, $J_{13}$ = 16), 6.83 (1H, d, $J$ = 12 Hz), 6.78 (1H, t, $J_{13}$ = 4 Hz), 6.66–6.64 (1H, dd, $J_{12}$ = 0.5.76 Hz), 5.23 (4H, $NH_2$, $CH_2$). Anal. found: C, 73.49; H, 5.06; N, 11.72. Calcd for $C_{22}H_{18}ClN_3$: C, 73.43; H, 5.04; N, 11.68.

**Synthesis of 1-(4-(3,4-diaminoquinolin-2-yl)phenyl)ethan-1-one (4b).** Light yellow semi-solid; yield 52%; IR (KBr, $cm^{-1}$): 3200 ($NH_2$ stretch), 1670 (C=O stretch), 1599 (C=N stretch), 1547. $^1$H NMR ($CDCl_3$, 400 MHz) $\delta$: 7.99 (2H, d, $J$ = 4 Hz), 7.70 (1H, d, $J$ = 4 Hz), 7.52 (2H, d, $J$ = 4 Hz), 7.21–7.18 (3H, m), 5.29 (4H, s) 2.75 (3H, s). HRMS (TOF-ESI) calcd for $C_{17}H_{15}N_3O$, 277.12 $(M)^+$; observed: 278.2189 $(M + H)^+$.

Physical data of unknown compounds **5a**, **5b**, **16** and **17** are given below.

**Synthesis of 2-(naphthalen-2-yl)quinolin-3-amine (5a).** Light yellow semi-solid; yield 67%; IR (KBr, $cm^{-1}$): 1600–1660 (naphthyl ring), 1250 (C–N stretch), 2982 (C–H stretch), 1547 (C=C aromatic). $^1$H NMR ($CDCl_3$, 400 MHz) $\delta$: 8.25 (1H, s), 8.06 (1H, d, $J$ = 1.6 Hz), 8.0 (1H, d, $J$ = 8 Hz), 7.9 (3H, m), 7.65 (1H, m), 7.55 (2H, m), 7.47 (3H, m); $^{13}$C NMR ($CDCl_3$, 100 MHz) $\delta$: 150.52, 142.78, 138.32, 137.19, 135.63, 133.67, 129.5, 129.34, 128.42, 128.45, 128.23, 128.21, 128.12, 127.87, 126.45, 125.45, 125.32, 116.67, 116.35; HRMS (TOF-ESI) calcd for $C_{19}H_{14}N_2$, 270.2 $(M)^+$; observed: 271.0839 $(M + H)^+$.

**Synthesis of 1-(4-(3-aminoquinolin-2-yl)phenyl)ethan-1-one (5b).** Light yellow semi-solid; yield 59%; IR (KBr, $cm^{-1}$): 2982 (C–H stretch), 1678 (C=O stretch), 1614 (C=N stretch), 1547 (C=C aromatic), 1264 (C–O stretch). $^1$H NMR ($CDCl_3$, 400 MHz) $\delta$: 8.10 (2H, dd, $J_{12}$ = 4 Hz), 7.99 (1H, dd, $J_{12}$ = 2.0 Hz), 7.88 (1H, dd, $J_{12}$ = 4 Hz), 7.62 (1H, dd, $J_{12}$ = 1.2 Hz), 7.48–7.44 (2H, m), 7.37 (1H, s), 2.66 (3H, s); HRMS (TOF-ESI) calcd for $C_{17}H_{14}N_2O$, 262.11 $(M)^+$; observed: 263.0510 $(M + H)^+$.

**Synthesis of 2-chloro-$N^4$-(2-methoxyphenyl)quinoline-3,4-diamine (16).** To a reaction vial, a suspension of 2-chloro-$N^4$-(2-methoxyphenyl)quinoline-3-amine (240 mg, 1 mmol) in methanol (1 mL) was added Sn/HCl (2 equiv.) and the mixture was refluxed for 6 h. After the completion of the reaction (TLC), methanol was evaporated. Compound was dried and purified through triturating with EtOAc and hexane mixture.

Yield: 42%, brown solid, mp: 169–170 °C.

$^1$H NMR ($CDCl_3$, 400 MHz, $\delta$ with TMS = 0): 8.79 (1H, d, $J$ = 2.4 Hz), 8.55 (2H, dd, $J_{12}$ = 2.4 Hz, $J_{13}$ = 4 Hz), 8.42 (1H, d, $J$ = 12), 8.26 (1H, $J$ = 2), 8.19 (1H, dd, $J_{12}$ = 2 Hz, $J_{13}$ = 8 Hz), 7.92–8.05 (1H, m), 7.06 (1H, d, $J$ = 8 Hz), 3.2 (3H, s). Anal. found: C, 64.31; H, 4.78; N, 14.06. Calcd for $C_{16}H_{14}ClN_3O$ : C, 64.11; H, 4.71; N, 14.02.

**Synthesis of 2-chloro-$N^4$-(3-chloro-4-flouro)quinoline-3,4-diamine (17).** To a reaction vial, a suspension of 2-chloro-*N*-(3-chloro-4-flouro)-3-nitroquinolin-4-amine (240 mg, 1 mmol) in methanol (1 mL) was added Sn/HCl (2 equiv.) and the mixture was refluxed for 6 h. After the completion of the reaction (TLC), methanol was evaporated. Compound was dried and purified through triturating with EtOAc and hexane mixture.

Yield: 32%, brown solid, mp: 170–172 °C.

$^1$H NMR ($CDCl_3$, 400 MHz, $\delta$ with TMS = 0): 7.84–7.88 (2H, m), 7.56–7.60 (1H, m), 7.34–7.39 (3H, m), 7.18–7.24 (3H, m). Anal. found: C, 55.90; H, 3.17; N, 13.02. Calcd for $C_{15}H_{10}C_{12}FN_3$: C, 55.92; H, 3.13; N, 13.04.

## Biological activity

**EGFR inhibitory assay.** To study the EGFR kinase inhibitory potential, the investigational compounds were screened for inhibition of ATP dependent phosphorylation of EGFR using z-lyte kinase assay kit-tyr4 peptide (Invitrogen; catalogue no. PV3193). This assay is based on an enzymatic reaction in which autophosphorylation and signaling activity of the epidermal growth factor receptor is measured. The inhibitory effect on kinase was measured spectrophotometrically at 400, 445 and 520 nm, respectively. Erlotinib was used as a positive control for the inhibition test. The reaction mixture consisted of 133 μL kinase buffer, 0.5 μL kinase peptide mixture, 0.5 μL phosphopeptide mixture, 0.5 μL ATP test sample solution (250 nM and 1, 5, 25 μM were dissolved in 4% DMSO). The assay plates were mixed and incubated at room temperature for 1 h (prepared in triplicates). Then, 5 μL of development solution was added into the mixture and mixed. The mixture was kept in dark for another 1 h. Next, the reaction was stopped with the addition of 5 μL stop solution. The absorbance was measured using UV-VIS spectrophotometer. Readings were taken in triplicate. Calculation emission ratio: emission ratio = coumarin emission (445 nm)/fluorescein emission (520 nm). The extent of phosphorylation was calculated by following formula:

$$\% \text{ phosphorylation} = 1 - \frac{(\text{emission ratio} \times F_{100\%}) - C_{100\%}}{(C_{0\%} - C_{100\%}) + [\text{emission ratio } (F_{100\%} - F_{0\%})]}$$

where $C_{0\%}$ = average coumarin emission signal of the 100% phos. control; $C_{100\%}$ = average coumarin emission signal of the 0% phos. control; $F_{100\%}$ = average fluorescein emission signal of the 100% phos. control; $F_{0\%}$ = average fluorescein emission signal of the 0% phos. control.

**RT-PCR and real time PCR.** Total RNA from the cells was isolated by Tri-reagent (Sigma-Aldrich) according to manufacturer's protocol. In brief, cells were lysed in Tri reagent by pipetting several times and mixed with chloroform and centrifuged at 12 000*g* for 10 minutes. The aqueous phase was removed and RNA was precipitated in isopropanol and pelletted at 10 000*g* for 10 minutes. The pellet was air dried and suspended in ultrapure water. cDNA was synthesized using 1 μg RNA as template in presence of MMLV-RT, MMLV-RT buffer, 10 mM dNTPs, DTT and RNAse OUT (Invitrogen).

Real time RT-PCR was performed by StepOnePlus thermal cycler system (Applied Biosystems) using double stranded DNA specific flurophore SYBR Green. Resolution of the product of interest from nonspecific product amplification was achieved by melt curve analysis.[44] Quantitation was performed with three different sets of cDNA samples. The list of primer used for RT and real time PCR is given below:

c-Fos (Fwd) – 5′ aaggagaatccgaagggaaa.
c-Fos (Rev) – 5′ agggcccttatgctcaatct.
Twist (Fwd) – 5′ *gtccgcagtcttacgaggag*.
Twist (Rev) – 5′ *ccagcttgagggtctgaatc*.
Actin (Fwd) – 5′ *agagctacgagctgcctgac*.
Actin (Rev) – 5′ *agcactgtgttggcgtacag*.

**Topoisomerase assays.** The topoisomerase inhibitory activity of investigated compounds was explored using drug screening kit bought from TopoGEN, Inc. (Columbus, OH).

**hTopo IIα mediated DNA decatenation assay.** In this assay, the reaction mixture contains 8 units hTopo IIα, 150 ng kDNA, 100 μM drug or test compound (dissolved in DMSO), freshly prepared 5× assay buffer and distilled $H_2O$. Assay buffer contains the mixture of buffer A (0.5 M Tris–HCl of pH 8, 1.5 M sodium chloride, 100 mM magnesium chloride, 5 mM dithiothreitol, 300 μg bovine serum albumin) and buffer B (20 mM ATP in water) in 1 : 1 ratio. All assay reactions were set up in the microcentrifuge tube. In assay components were added in order given as assay buffer, kDNA, inhibitor and then reaction was started by adding hTopo IIα. Final reaction volume was adjusted to 20 μL using distilled water and incubation was made at 37 °C for 30 min. Next, the reaction was halted by addition of 10% SDS and proteinase K. Formed decatenation products were separated by running agarose gel (1%) electrophoresis in Tris–acetate–EDTA (TAE) buffer containing 0.5 μg $mL^{-1}$ ethidium bromide. Gel was subjected to destaining for 20 minutes in distilled water. Decatenated products formed were photographed by Gel Doc EZ imager (BioRad, USA) and quantitated by using ImageLab (BioRad).

**hTopo I mediated DNA relaxation assay.** In hTopoI mediated DNA relaxation assay, reaction mixture comprises of 10× assay buffer (100 mM Tris–HCl of pH 7.9, 10 mM EDTA, 1.5 M sodium chloride, 1% BSA, 1 mM spermidine, 50% glycerol), 250 ng supercoiled DNA as a substrate, 100 μM camptothecin or investigational compound (dissolved in DMSO) then distilled water used to make final volume up to 20 μL. The reaction was initiated by incubating with purified hTopoI at 37 °C for 30 min. The reaction was terminated by the addition of 10% SDS and proteinase K followed by incubation for 15 min at 70 °C. Relaxed isoforms were distinguished by agarose gel (1%) electrophoresis in Tris–acetate–EDTA (TAE) buffer encompassing 0.5 μg $mL^{-1}$ ethidium bromide.

The bands were pictured by Gel Doc EZ imager (BioRad, U. S. A.) and analyzed using ImageLab (BioRad).

## Molecular docking study

The 3D co-crystal structures of EGFR with erlotinib (PDB entry: 1M17)[29] and human topoisomerase IIα with ANP (PDB entry: 1ZXM)[38] were procured from the protein data bank. The 2D structures of the compounds were drawn using ChemBioDraw Ultra 12.0 and the energy minimization was done using the MM2 force field. The ligands were neutralized and desalt using the Ligprep module. The protein preparation was carried out using the Protein Preparation Wizard in Maestro 9.6. Correction of the raw PDB structure included; addition of hydrogen atoms, assigning bond orders, removal of water molecules beyond 5 Å, assigning formal charges and filling the missing side chain and loops using PRIME. Further, the optimization and refinement of the pre-processed protein structure were done using the OPLS-2005 force field. The grid was generated around the centroid of the co-crystallized ligand; ANP for Topo IIα and erlotinib in the case of EGFR. The docking was performed using GLIDE extra precision (XP) module.

## Cell culture and treatment

All the cell lines were procured from National cell repository situated at NCCS, Pune. Lung (A-549 and H-460), prostate (PC-3) and colon (HCT-116-wild type and HCT-116-p53 null) cancer cell lines representing different human cancers were grown in DMEM media accompanied with 10% fetal bovine serum (FBS) and antibiotic solution (1× Penstrip, Invitrogen). The cells were incubated at 37 °C with 5% $CO_2$ and 95% humidity conditions. For experiments, cells were seeded in equal numbers after trypan blue cell counting (5000–8000 cells per well of 96-well plate). Afterwards cells were washed once with sterile 1× PBS and cultured with serum free media for 24 h for synchronization. The test compounds were dissolved in cell culture grade DMSO. The total amount of media per well (100 μL per well of 96 well plate) was kept constant and all the treatment volumes were accommodated within these ranges only.

## 3-(4,5-Dimethythiazol-2-yl)-2,5-diphenyl tetrazolium bromide (MTT) assay

MTT assay was done using 96-well plate; each well was filled by 100 μL media to which cell were treated with the synthetic compounds for 48 h.[21] After 48 h media was discarded and subsequently washed with 1× PBS and were consequently

 

treated with MTT dye (5 mg in 10 mL of 1× PBS) at a concentration of 10 μL per well and incubated at room temperature in dark for 4 h to allow formation of formazan crystals. After 4 h crystals so formed were dissolved thoroughly using DMSO (100 μL). This was followed by readings using microplate reader at 570 nm. The results were then represented as mean ± S.D. obtained from three independent experiments.

### Human peripheral blood mononuclear cells (PBMCs) culture and MTT assay

5 mL of fresh blood was drawn from healthy individual as per the protocol no. CUPB/cc/14/IEC/4483 approved by Institutional Ethics Committee of Central University of Punjab, Bathinda. The protocol used was standard operating procedure, provided by Institutional Ethics Committee of Central University of Punjab according to guidelines issued by Indian Council of Medical Research (ICMR), Govt. of India. Human peripheral blood mononuclear cells (PBMCs) were isolated from whole blood discarding the RBCs after treatment with RBC lysis buffer. The cells were then suspended in RPMI media supplemented with 10% fetal bovine serum (FBS), 1× antibiotic solution and were incubated at 37 °C with 5% $CO_2$ and 95% humidity.

The PBMCs were counted on the automated cell counter (Invitrogen). Approximately 10 000 cells were seeded in each well of the 96 well plate. The treatment was given to the cells in triplicate at different concentrations for 48 h. The MTT solution (4 mg $mL^{-1}$) was than added to the cells and incubated for 4 h in dark. The resultant intracellular precipitate (formazan) thus formed was dissolved in DMSO solution and the absorbance was read spectrometrically at 570 nm.

### Reactive oxygen species (ROS) and mitochondrial membrane integrity assays

24 h post treatment, the cells were processed for JC-1 or DHE staining. Cells were stained with DHE at 37 °C for 30 minutes followed by measuring of the OD at 610 nm using a microplate reader after washing with 1× PBS to remove excess dye. For the JC-1 assay, dye was directly added to the media and cells were incubated at 37 °C for 30 minutes, followed by washing with 1× PBS to remove extra dye. The OD was measured using a microplate reader (emission at 527 and 590).[15]

### Cell apoptosis assay (using annexin V)

Apoptosis utilising Muse™ Annexin V and Dead Cell kit (catalogue no. 15-0180) was performed using Muse™ cell analyzer. Cellular samples (A549 previously treated with compound **3m** for 24 h) were prepared by the predefined protocol of Muse™ Annexin V and Dead Cell kit. The total cells and media were centrifuged at 1200 rpm for 5 min and washed with 1× PBS. 50 μL of kit reagent was added and incubated for 30 minutes at room temperature in dark before the analysis.

### Cell cycle analysis

Cell cycle analysis was performed using flow cytometry (BD Accuri). Cellular samples (A549 previously treated with compound **3m** for 24 h) were prepared for staining by transferring $1 \times 10^5$ to $1 \times 10^6$ cells to each tube. Then cell was centrifuged at 1200 rpm for 5 min and washed with 1× PBS. The cells were then suspended using chilled ethanol and the cell concentration thereby raised to $5 \times 10^5$ to $1 \times 10^6$ cells per mL. The cells were then incubated for 3 h at −20 °C. Then 200 μL of fixed cells were added to new tube. Then they were subjected to centrifugation at 2500 rpm and washed once with 1× PBS. 50 μL of propidium iodide (along with 50 μL ribonuclease A) was added to each well and incubated for 30 minutes at room temperature in dark.

The A549 cell lines treated with compound **3m** previously for 48 h were harvested using the above mentioned protocol. Instead of propidium iodide Muse™ cell cycle reagent (catalogue no. 15-0172) was added to each tube and incubated for 30 minutes at room temperature in the dark. The DNA content was then measured using Muse™ flow cytometer.

## Acknowledgements

RK, MC and GJ thank DST and UGC, New Delhi, India for the financial assistance (F. no. SR/FT/CS-71/2011) and F.30-13/2013 (BSR), respectively. SS thanks DST for financial assistance (DST-SERB EMR, SR/SO/AS-31/2014), PS is recipient of JRF from the project. SMA, KDB and UCB are thankful to DBT, New Delhi and NIPER, S.A.S. Nagar for financial support.

## References

1 D. R. Robinson, Y.-M. Wu and S.-F. Lin, *Oncogene*, 2000, **19**, 5548–5557.
2 M. A. Lemmon and J. Schlessinger, *Cell*, 2010, **141**, 1117–1134.
3 J. T. Hartmann, M. Haap, H.-G. Kopp and H.-P. Lipp, *Curr. Drug Metab.*, 2009, **10**, 470–481.
4 A. Levitzki, *Annu. Rev. Pharmacol. Toxicol.*, 2013, **53**, 161–185.
5 O. Cruz-Lopez, A. Conejo-García, M. C. Nunez, M. Kimatrai, M. E. Garcia-Rubino, F. Morales, V. Gomez-Perez and J. M. Campos, *Curr. Med. Chem.*, 2011, **18**, 943–963.
6 F. Buron, J. Merour, M. Akssira, G. Guillaumet and S. Routier, *Eur. J. Med. Chem.*, 2015, **95**, 76–95.
7 T. Asano, T. Yoshikawa, T. Usui, H. Yamamoto, Y. Yamamoto, Y. Uehara and H. Nakamura, *Bioorg. Med. Chem.*, 2004, **12**, 3529–3542.
8 C. R. Prakash and S. Raja, *Mini-Rev. Med. Chem.*, 2012, **12**, 98–119.
9 H. Mastalerz, M. Chang, P. Chen, P. Dextraze, B. E. Fink, A. Gavai, B. Goyal, W.-C. Han, W. Johnson, D. Langley and F. Y. Lee, *Bioorg. Med. Chem. Lett.*, 2007, **17**, 2036–2042.
10 M. Chauhan, G. Sharma, G. Joshi and R. Kumar, *Curr. Pharm. Des.*, 2016, **22**, 3226–3236.
11 D. B. Khadka and W.-J. Cho, *Expert Opin. Ther. Pat.*, 2013, **23**, 1033–1056.

12 Y. Pommier, *Nat. Rev. Cancer*, 2006, **6**, 789–802.
13 Y. Pommier, E. Leo, H. Zhang and C. Marchand, *Chem. Biol.*, 2010, **17**, 421–433.
14 N. Yoshimura, S. Kudoh, T. Kimura, S. Mitsuoka, K. Matsuura, K. Hirata, K. Matsui, S. Negoro, K. Nakagawa and M. Fukuoka, *Lung Cancer*, 2006, **51**, 363–368.
15 J. M. Alex, S. Singh and R. Kumar, *Arch. Pharm.*, 2014, **347**, 717–727.
16 A. T. Baviskar, U. C. Banerjee, M. Gupta, R. Singh, S. Kumar, M. K. Gupta, S. Kumar, S. K. Raut, M. Khullar, S. Singh and R. Kumar, *Bioorg. Med. Chem.*, 2013, **21**, 5782–5793.
17 M. Chauhan, A. Rana, J. M. Alex, A. Negi, S. Singh and R. Kumar, *Bioorg. Chem.*, 2015, **58**, 1–10.
18 G. Joshi, P. K. Singh, A. Negi, A. Rana, S. Singh and R. Kumar, *Chem.-Biol. Interact.*, 2015, **240**, 120–133.
19 G. Kaur, R. P. Cholia, A. K. Mantha and R. Kumar, *J. Med. Chem.*, 2014, **57**, 10241–10256.
20 A. Kondaskar, S. Kondaskar, R. Kumar, J. C. Fishbein, N. Muvarak, R. G. Lapidus, M. Sadowska, M. J. Edelman, G. M. Bol, F. Vesuna and V. Raman, *ACS Med. Chem. Lett.*, 2010, **2**, 252–256.
21 Darpan, G. Joshi, S. M. Amrutkar, A. T. Bhaviskar, H. Kler, S. Singh, U. C. Banerjee and R. Kumar, *RSC Adv.*, 2016, **6**, 14880–14892.
22 S. Kumar, S. Sapra, R. Kumar, M. K. Gupta, S. Koul, T. Kour, A. K. Saxena, O. P. Suri and K. L. Dhar, *Med. Chem. Res.*, 2012, **21**, 3720–3729.
23 A. Negi, J. M. Alex, S. M. Amrutkar, A. T. Baviskar, G. Joshi, S. Singh, U. C. Banerjee and R. Kumar, *Bioorg. Med. Chem.*, 2015, **23**, 5654–5661.
24 A. Rana, J. M. Alex, M. Chauhan, G. Joshi and R. Kumar, *Med. Chem. Res.*, 2015, **24**, 903–920.
25 S. S. Malhi, A. Budhiraja, S. Arora, K. R. Chaudhari, K. Nepali, R. Kumar, H. Sohi and R. S. Murthy, *Int. J. Pharm.*, 2012, **432**, 63–74.
26 H. F. Motiwala, R. Kumar and A. K. Chakraborti, *Aust. J. Chem.*, 2007, **60**, 369–374.
27 M. Z. Hernandes, S. M. T. Cavalcanti, D. R. M. Moreira, J. de Azevedo, W. Filgueira and A. C. L. Leite, *Curr. Drug Targets*, 2010, **11**, 303–314.
28 L. A. Hardegger, B. Kuhn, B. Spinnler, L. Anselm, R. Ecabert, M. Stihle, B. Gsell, R. Thoma, J. Diez and J. Benz, *Angew. Chem., Int. Ed.*, 2011, **50**, 314–318.
29 J. Stamos, M. X. Sliwkowski and C. Eigenbrot, *J. Biol. Chem.*, 2002, **277**, 46265–46272.
30 J. R. Sierra, V. Cepero and S. Giordano, *Mol. Cancer*, 2010, **9**, 75.
31 G. R. Oxnard, M. E. Arcila, C. S. Sima, G. J. Riely, J. Chmielecki, M. G. Kris, W. Pao, M. Ladanyi and V. A. Miller, *Clin. Cancer Res.*, 2011, **17**, 1616–1622.
32 H.-H. Li, H. Huang, X.-h. Zhang, X.-m. Luo, L.-p. Lin, H.-l. Jiang, J. Ding, K.-x. Chen and H. Liu, *Acta Pharmacol. Sin.*, 2008, **29**, 1529–1538.
33 H.-W. Lo, S.-C. Hsu, W. Xia, X. Cao, J.-Y. Shih, Y. Wei, J. L. Abbruzzese, G. N. Hortobagyi and M.-C. Hung, *Cancer Res.*, 2007, **67**, 9066–9076.
34 A. Jimeno, P. Kulesza, E. Kincaid, N. Bouaroud, A. Chan, A. Forastiere, J. Brahmer, D. P. Clark and M. Hidalgo, *Cancer Res.*, 2006, **66**, 2385–2390.
35 R. Peleg, D. Bobilev and E. Priel, *Int. J. Oncol.*, 2014, **44**, 934–942.
36 S. Jiménez-Alonso, H. C. Orellana, A. Estevez-Braun, A. G. Ravelo, E. Perez-Sacau and F. Machin, *J. Med. Chem.*, 2008, **51**, 6761–6772.
37 P. Arthi, S. Shobana, P. Srinivasan, D. Prabhu, C. Arulvasu and A. K. Rahiman, *J. Photochem. Photobiol., B*, 2015, **153**, 247–260.
38 H. Wei, A. J. Ruthenburg, S. K. Bechis and G. L. Verdine, *J. Biol. Chem.*, 2005, **280**, 37041–37047.
39 Y. Yang, S. Karakhanova, J. Werner and A. V. Bazhin, *Curr. Med. Chem.*, 2013, **20**, 3677–3692.
40 M. Benhar, D. Engelberg and A. Levitzki, *EMBO Rep.*, 2002, **3**, 420–425.
41 G.-Y. Liou and P. Storz, *Free Radical Res.*, 2010, **44**, 479–496.
42 A. Perelman, C. Wachtel, M. Cohen, S. Haupt, H. Shapiro and A. Tzur, *Cell Death Dis.*, 2012, **3**, e430.
43 J. Massague, *Nature*, 2004, **432**, 298–306.
44 L. Pavithra, S. Singh, K. Sreenath and S. Chattopadhyay, *Int. J. Biochem. Cell Biol.*, 2009, **41**, 862–871.

 